University of Alberta

Numerical Characterization of Ultrasound Elastography for the Early Detection of Deep Tissue Injuries

by

Kenton Hamaluik

A thesis submitted to the Faculty of Graduate Studies and Research in partial fulfilment of the requirements for the degree of

Master of Science

Department of Mechanical Engineering

Fall 2013
Edmonton, Alberta

Abstract

[c1]Deep tissue injuries are subcutaneous regions of extreme tissue breakdown generally induced by the application of significant mechanical pressure over extended periods of time through the biological mechanisms of ischemia and cell deformation causing rupture. These wounds are commonly suffered as a secondary wound or disease, often formed due to extended periods of motionless such as stationary sitting in spinal cord injured patients or those undergoing surgery. [c2]

[c1] *KH*: Way too long

[c2] *KH*: Abstract should be <= 150 words and give a decent summary of everything

Acknowledgements

Lorem ipsum dolor sit amet, consectetuer adipiscing elit. Ut purus elit, vestibulum ut, placerat ac, adipiscing vitae, felis. Curabitur dictum gravida mauris. Nam arcu libero, nonummy eget, consectetuer id, vulputate a, magna. Donec vehicula augue eu neque. Pellentesque habitant morbi tristique senectus et netus et malesuada fames ac turpis egestas. Mauris ut leo. Cras viverra metus rhoncus sem. Nulla et lectus vestibulum urna fringilla ultrices. Phasellus eu tellus sit amet tortor gravida placerat. Integer sapien est, iaculis in, pretium quis, viverra ac, nunc. Praesent eget sem vel leo ultrices bibendum. Aenean faucibus. Morbi dolor nulla, malesuada eu, pulvinar at, mollis ac, nulla. Curabitur auctor semper nulla. Donec varius orci eget risus. Duis nibh mi, congue eu, accumsan eleifend, sagittis quis, diam. Duis eget orci sit amet orci dignissim rutrum.

Contents

List of Tables

List of Figures

Chapter 1

Introduction

1.1 Motivation

Pressure ulcers are debilitating wounds often suffered by people with limited mobility such as those undergoing lengthy surgical procedures, the elderly, and those with spinal cord injuries (SCI) [1]—up to 80 % of people with SCI will develop a pressure ulcer in their lifetime [2]. Pressure ulcers are generally characterized by a deterioration of the skin leading to painful open wounds and while many pressure ulcers may be blamed on excess friction and moisture at the skin surface, many can start as "deep tissue injuries" (DTI) which start deep below the skin surface—most often at the bone-muscle interface [3]. DTI are generally thought to be formed due to some combination of excessive deformation and ischemia resulting from sustained loading on localized tissue [4]–[6]. As of the time of writing, there is no clinically feasible method of detecting deep tissue injuries until they begin to damage the skin—even the National Pressure Ulcer Advisory Panel's description of them is largely based on their appearance after the fact [7]. With our inability to detect these forming injuries and subsequently implement deep tissue injury prevention

and mitigation protocols, the injuries may eventually progress to form large subcutaneous cavities which eventually break through the surface and reveal themselves as stage III or IV pressure ulcers [8], [9].

Currently, the only tool capable of readily detecting early deep tissue injuries is T_2-weighted MRI [6], [10]. Unfortunately, MRI is not cost-effective for detecting the onset of DTI in a clinical population. Alternately, ultrasound is a much more cost-effective, if less sensitive imaging modality. While it has been shown that some DTI may be discerned using classical b-mode ultrasound imaging [3], [11], the sonographic features of DTI are difficult to separate from regular tissue inhomogeneities. To overcome this, ultrasound elastography may provide more reliable results by imaging the mechanical tissue stiffness rather than its acoustic properties. Ultrasound elastography is an imaging modality that utilizes sonographic techniques to determine the localized mechanical stiffness of tissue and is currently used clinically to detect breast and prostate cancer lesions [12], [13] as well as liver fibrosis [14]. It is known that as DTI form, they undergo mechanical stiffness changes throughout their progression [9], [15], [16], with tissue undergoing significant 1.8 – 3.3-fold mechanical stiffening during injury formation [5]. Initially damaged tissues show signs of increased relative stiffness due to edema-related swelling, while eventually showing signs of decreased relative stiffness due to decomposition and necrosis [17]. Since ultrasound elastography is capable of imaging these stiffness changes, it follows that the formation and progression of DTI may be imaged using ultrasound elastography. In fact, ultrasound elastography has shown to be a valid technique for imaging the formation of a DTI in a rat model [18]. Before this technique can be fully understood and used in human patients, the various parameters involved in performing ultrasound elastography must be characterized with respect to detecting DTI in humans.

1.2 Objective

The broad objective of this work was to numerically characterize the use of ultrasound elastography to detect and monitor formative and progressive deep tissue injuries. Although it has been shown that ultrasound elastography is capable of imaging DTI [18], the degree of suitability of this technique with regard to DTI is not yet understood. When the effect of numerous interrogation parameters on detection sensitivity and ability is known, the technology may be evaluated on its feasibility and usefulness to detect deep tissue injuries. The ultimate goal of this characterization is to be the first stage in the process of allowing ultrasound elastography to be implemented clinically for detecting DTI. It is reasoned that if early detection modalities are implemented clinically, both patients and the health care system may benefit by lowering the incidence and outright cost of treating fully-formed deep tissue injuries.

1.3 Methodology

In order to investigate the use of ultrasound elastography for the detection of deep tissue injuries, the technology must first be characterized and fully understood. While traditional experimentation provides an opportunity to work with physical subjects it can be severely limiting as absolute control over all investigated parameters is relinquished. Further, subject recruitment may present an insurmountable barrier to the execution of such a study. As such, in this exploratory work, various numerical models of the technology have been utilized to investigate the controlled effect of a broad number of parameters relating to each technology. Specifically, k-space models of ultrasonic wave propagation and finite-element models of tissue deformation have been developed. These models were coupled with tissue strain estimation algorithms to

fully simulate the ultrasound ultrasound elastography procedures. Parametric studies on the detection sensitivity and ability of the various ultrasound elastography procedures were carried out with respect to various lesion and technological parameters. Chief parameters of interest included those related to the physical realities of deep tissue injuries such as lesion depth, size, and relative mechanical stiffness as well as parameters related to the design and development of appropriate ultrasonic transducers such as probing frequency, transducer f-number, etc.

1.4 Thesis Outline

In this work, three methods of ultrasonic elastogram image formation have been investigated: quasi-static ultrasound elastography, acoustic radiation force impulse imaging, and shear wave speed quantification. While all three methods may be used to interrogate tissue stiffness, each does so in a distinctively unique way. The academic background leading to the motivation for this work and the development of the numerical models is presented in Chapter 2.

Quasi-static ultrasound elastography estimates tissue strain by tracking inhomogeneities across pre- and post- compression b-mode scans where the compression is generated by manual indentation of the transducer against the surface of the skin. To investigate this technique, two-dimensional b-mode ultrasound scans of simulated pre- and post-compression tissue were generated. A finite-element model of tissue deformation was utilized to generate the post-compression simulated scans. A published tissue strain estimation algorithm was utilized to then generate elastograms for the parametric study. The models and results are presented in Chapter 3.

blurb about ARFI here..

blurb about shear here..

Finally, the results presented in this work and their implications along with suggestions for future work are discussed in Chapter 6.

References

[1] R. M. Allman, P. S. Goode, M. M. Patrick, N. Burst, and A. A. Bartolucci, "Pressure ulcer risk factors among hospitalized patients with activity limitation.," *JAMA : the journal of the American Medical Association*, vol. 273, no. 11, pp. 865–870, Mar. 15, 1995, ISSN: 0098-7484. [Online]. Available: http://view.ncbi.nlm.nih.gov/pubmed/7869557.

[2] C. A. Salzberg, D. W. Byrne, C. G. Cayten, P. van Niewerburgh, J. G. Murphy, and M. Viehbeck, "A new pressure ulcer risk assessment scale for individuals with spinal cord injury.," *American journal of physical medicine & rehabilitation / Association of Academic Physiatrists*, vol. 75, no. 2, pp. 96–104, 1996, ISSN: 0894-9115. [Online]. Available: http://view.ncbi.nlm.nih.gov/pubmed/8630201.

[3] N. Kanno, T. Nakamura, M. Yamanaka, K. Kouda, T. Nakamura, and F. Tajima, "Low-echoic lesions underneath the skin in subjects with spinal-cord injury.," *Spinal cord*, vol. 47, no. 3, pp. 225–229, Mar. 2009, ISSN: 1362-4393. DOI: 10.1038/sc.2008.101. [Online]. Available: http://dx.doi.org/10.1038/sc.2008.101.

[4] A. Stekelenburg, D. Gawlitta, D. L. Bader, and C. W. Oomens, "Deep tissue injury: how deep is our understanding?" *Archives of physical medicine and rehabilitation*, vol. 89, no. 7, pp. 1410–1413, Jul. 2008, ISSN: 1532-821X. DOI: 10.1016/j.apmr.2008.01.012. [Online]. Available: http://dx.doi.org/10.1016/j.apmr.2008.01.012.

[5] A. Gefen, N. Gefen, E. Linder-Ganz, and S. S. Margulies, "In vivo muscle stiffening under bone compression promotes deep pressure sores.," *Journal of biomechanical engineering*, vol. 127, no. 3, pp. 512–524, Jun.

2005, ISSN: 0148-0731. [Online]. Available: http://view.ncbi.nlm.nih.gov/pubmed/16060358.

[6] S. Loerakker, E. Manders, G. J. Strijkers, K. Nicolay, F. P. Baaijens, D. L. Bader, and C. W. Oomens, "The effects of deformation, ischemia, and reperfusion on the development of muscle damage during prolonged loading.," *Journal of applied physiology (Bethesda, Md. : 1985)*, vol. 111, no. 4, pp. 1168–1177, Oct. 14, 2011, ISSN: 1522-1601. DOI: 10.1152/japplphysiol.00389.2011. [Online]. Available: http://dx.doi.org/10.1152/japplphysiol.00389.2011.

[7] J. Black, M. M. M. Baharestani, J. Cuddigan, B. Dorner, L. Edsberg, D. Langemo, M. E. E. Posthauer, C. Ratliff, G. Taler, and National Pressure Ulcer Advisory Panel, "National pressure ulcer advisory panel's updated pressure ulcer staging system.," *Advances in skin & wound care*, vol. 20, no. 5, pp. 269–274, May 2007, ISSN: 1527-7941. DOI: 10.1097/01.asw.0000269314.23015.e9. [Online]. Available: http://dx.doi.org/10.1097/01.asw.0000269314.23015.e9.

[8] C. V. Bouten, C. W. Oomens, F. P. Baaijens, and D. L. Bader, "The etiology of pressure ulcers: skin deep or muscle bound?" *Archives of physical medicine and rehabilitation*, vol. 84, no. 4, pp. 616–619, Apr. 2003, ISSN: 0003-9993. DOI: 10.1053/apmr.2003.50038. [Online]. Available: http://dx.doi.org/10.1053/apmr.2003.50038.

[9] C. W. Oomens, S. Loerakker, and D. L. Bader, "The importance of internal strain as opposed to interface pressure in the prevention of pressure related deep tissue injury.," *Journal of tissue viability*, vol. 19, no. 2, pp. 35–42, May 2010, ISSN: 0965-206X. DOI: 10.1016/j.jtv.2009.11.

002. [Online]. Available: http://dx.doi.org/10.1016/j.jtv.2009.11.002.

[10] A. Stekelenburg, C. W. Oomens, G. J. Strijkers, K. Nicolay, and D. L. Bader, "Compression-induced deep tissue injury examined with magnetic resonance imaging and histology.," *Journal of applied physiology (Bethesda, Md. : 1985)*, vol. 100, no. 6, pp. 1946–1954, Jun. 2006, ISSN: 8750-7587. DOI: 10.1152/japplphysiol.00889.2005. [Online]. Available: http://dx.doi.org/10.1152/japplphysiol.00889.2005.

[11] N. Aoi, K. Yoshimura, T. Kadono, G. Nakagami, S. Iizuka, T. Higashino, J. Araki, I. Koshima, and H. Sanada, "Ultrasound assessment of deep tissue injury in pressure ulcers: possible prediction of pressure ulcer progression.," *Plastic and reconstructive surgery*, vol. 124, no. 2, pp. 540–550, Aug. 2009, ISSN: 1529-4242. DOI: 10.1097/prs.0b013e3181addb33. [Online]. Available: http://dx.doi.org/10.1097/prs.0b013e3181addb33.

[12] M. Tanter, J. Bercoff, A. Athanasiou, T. Deffieux, J.-L. L. Gennisson, G. Montaldo, M. Muller, A. Tardivon, and M. Fink, "Quantitative assessment of breast lesion viscoelasticity: initial clinical results using supersonic shear imaging.," *Ultrasound in medicine & biology*, vol. 34, no. 9, pp. 1373–1386, Sep. 2008, ISSN: 0301-5629. DOI: 10.1016/j.ultrasmedbio.2008.02.002. [Online]. Available: http://dx.doi.org/10.1016/j.ultrasmedbio.2008.02.002.

[13] K. König, U. Scheipers, A. Pesavento, A. Lorenz, H. Ermert, and T. Senge, "Initial experiences with real-time elastography guided biopsies of the prostate.," *The Journal of urology*, vol. 174, no. 1, pp. 115–117, Jul. 2005, ISSN: 0022-5347. DOI: 10.1097/01.ju.0000162043.72294.4a.

[Online]. Available: http://dx.doi.org/10.1097/01.ju.0000162043.72294.4a.

[14] L. Sandrin, B. Fourquet, J.-M. M. Hasquenoph, S. Yon, C. Fournier, F. Mal, C. Christidis, M. Ziol, B. Poulet, F. Kazemi, M. Beaugrand, and R. Palau, "Transient elastography: a new noninvasive method for assessment of hepatic fibrosis.," *Ultrasound in medicine & biology*, vol. 29, no. 12, pp. 1705–1713, Dec. 2003, ISSN: 0301-5629. [Online]. Available: http://view.ncbi.nlm.nih.gov/pubmed/14698338.

[15] E. Linder-Ganz and A. Gefen, "Mechanical compression-induced pressure sores in rat hindlimb: muscle stiffness, histology, and computational models.," *Journal of applied physiology (Bethesda, Md. : 1985)*, vol. 96, no. 6, pp. 2034–2049, Jun. 2004, ISSN: 8750-7587. DOI: 10.1152/japplphysiol.00888.2003. [Online]. Available: http://dx.doi.org/10.1152/japplphysiol.00888.2003.

[16] L. R. Solis, A. B. Liggins, P. Seres, R. R. Uwiera, N. R. Poppe, E. Pehowich, R. B. Thompson, and V. K. Mushahwar, "Distribution of internal strains around bony prominences in pigs.," *Annals of biomedical engineering*, pp. 1–19, Mar. 8, 2012, ISSN: 1521-6047. DOI: 10.1007/s10439-012-0539-y. [Online]. Available: http://dx.doi.org/10.1007/s10439-012-0539-y.

[17] A. Gefen, "Deep tissue injury from a bioengineering point of view.," *Ostomy/wound management*, vol. 55, no. 4, pp. 26–36, Apr. 2009, ISSN: 0889-5899. [Online]. Available: http://view.ncbi.nlm.nih.gov/pubmed/19387094.

[18] J.-F. F. Deprez, E. Brusseau, J. Fromageau, G. Cloutier, and O. Basset, "On the potential of ultrasound elastography for pressure ulcer early

detection.," *Medical physics*, vol. 38, no. 4, pp. 1943–1950, Apr. 2011, ISSN: 0094-2405. [Online]. Available: http://view.ncbi.nlm.nih.gov/pubmed/21626927.

Chapter 2

Literature Review

2.1 Introduction

[c1]Pressure ulcers are an extraordinarily large problem facing the health care system today. Not only are billions of dollars spent annually treating these injuries but they also place an extremely significant burden on the people who suffer from them. Deep tissue injuries are currently considered a subset of pressure ulcers, although it is hypothesized that due to a lack of clinical detection modalities, most deep tissue injuries go undiagnosed until they characteristically "break through" the surface of the skin, at which point they are diagnosed as stage III or IV ulcers instead of an advanced deep tissue injury. While deep tissue injury prevention and mitigation strategies exist, the lack of a substantial method of detecting and diagnosing these injuries leads to an overall lack of coordination and sub-par treatment outcomes. The inclusion of a viable means of detecting early deep tissue injuries can only serve to strengthen the prevention and mitigation strategies that exist and give not only health-care practitioners but also researchers a solid foundation to base their treatments off of.

[c1] *KH*: Should this maybe go in the introduction chapter? If so, what should go here?

2.2 Deep Tissue Injuries

According to the National Pressure Ulcer Advisory staging system, deep tissue injuries are defined as a "purple or maroon localized area of discolored intact skin or blood-filled blister due to damage of underlying soft tissue from pressure and / or shear" [1]. The definition goes on to say that "the area may be preceded by tissue that is painful, firm, mushy, boggy, warmer, or cooler as compared to to adjacent tissue." This definition is somewhat vague, however, and the exact aetiology of this injuries will be discussed in detail in Section 2.2.1. Gunningberg et al. suggest that in order to reduce the prevalence of pressure ulcers, skin and risk assessment should be done as early as possible [2].

- Hospital-acquired pressure ulcers: a comparison of costs in medical vs. surgical patients [3]
- Pressure ulcer research funding in America: creation and analysis of an on-line database [4]
- Pressure ulcers in America: prevalence, incidence, and implications for the future. An executive summary of the National Pressure Ulcer Advisory Panel monograph [5]
- Hospitalzations related to pressure ulcers among adults 18 years and older, 2006: statistical brief no. 64 [6]
- Pressure ulcers in the elderly: analysis of prevalence and risk factors [7]
- Assessment and management of pressure ulcers in the elderly: current strategies [8]
- Pressure ulcers: the great insult [9]

- Reducing pressure ulcer prevalence rates in the long-term acute care setting [10]
- In-hopsital medical complications, length of stay, and mortality among stroke unit patients [11]
- Tracking quality over time: what do pressure ulcer data show? [2]
- Recurrence of initial pressure ulcer in persons with spinal cord injuries [12]

2.2.1 Aetiology and Histology

Deep tissue injuries are regions of subcutaneous tissue breakdown characterized by severe necrosis of the tissue. These injuries most commonly form immediately superior to boney prominences and gradually "tunnel" towards the surface of the skin. Upon superficial rupture, the wound is characterized by "full thickness tissue loss" with slough or eschar potentially present.

Deep tissue injuries are thought to occur through the combinatory effects of two distinct but related mechanisms: ischemia and cell deformation. Ischemia is a condition where the blood supply to tissue has been cut off, rendering the tissue unable to function appropriately. Cell deformation occurs when mechanical strains are imparted upon the tissue, causing excessive deformation in not only the extracellular matrix, but in the cells as well. Taken together, the presence of these two factors has been shown to greatly increase the risk of developing a deep tissue injury [13].

For quite some time, ischemia was regarded as the chief acute risk factor for developing late-stage pressure ulcers [14], [15]. Studies showed that although tissue was able to survive complete ischemia for approximately 4 hours before severe necrosis set in [16].

Later, ischemia-induced reperfusion injury was implicated in the formation of DTI [17]–[19]. An ischemia-induced reperfusion injury is caused when blood is allowed to flow back into a region of tissue that was previously ischemic. While seeming somewhat contrary to its expected effect, the restoration of circulation results in a swelling and inflammatory effect which causes great microvascular damage [18]. The effect of reperfusion was confirmed when comparing pure ischemic conditions in tissue to a cycle of ischemic-reperfused conditions over the same period of time, where it was found that significantly greater damage was caused by repeated loading-unloading rather than simple constant loading [19].

- Compression induced damage and internal tissue strains are related [20]. With a combined animal-experimental numerical approach, we show that there is a reproducible monotonic
- Microstructural analusis of deformation-induced hypoxic damage in skeletal muscle [21]
- How does muscle stiffness affect the internal deformatins within the soft tissue layers of the buttocks under constant loading? [22]
- A theoretical model to study the effects of cellular stiffening on the damage eveolution in deep tissue injury [23]
- The biomechanics of sitting-acquired pressure ulcers in patients with spinal cord injury or lesions [24]
- Assessment of mechanical conditions in sub-dermal tissues during sitting: a combined expeirmental-MRI and finite-element approach [25]
- Mechanical gluteal soft tissue material parameter validation under complex tissue loading [26]

- Diffusion of water in skeletal muscle tissue is not influenced by compression in a rat model of deep tissue injury [27].
- Pressure ulcer risk factors among hospitalized patients with activity limitation [28]
- The etiology of pressure ulcers: skin deep or muscle bound? [29]
- Histopathology of pressure ulcers as a result of sequential computer-controller pressure sessions in a fuzzy rat model [30]
- National Pressure Ulcer Advisory Panel's Updated Pressure Ulcer Staging System [31]
- Diffusion of ulcers in the diabetic foot is promoted by stiffening of plantar muscular tissue under excessive bone compression [32]
- Risk factors for a pressure-related deep tissue injury: a theoretical mode [33]
- Deep tissue injury: how deep is our understanding? [13]
- Deep tissue injury from a bioengineering point of view [34]
- Distribution of internal pressure around bony prominences: implications to deep tissue injury and effectiveness of intermittent electrical stimulation [35]
- Distribution of internal strains around bony prominences in pigs [36]
- The importance of internal strain as opposed to interface pressure in the prevention of pressure related deep tissue injury [37]
- Stress analyses coupled with damage laws to determine biomechanical risk factors for deep tissue injury during sitting [38]

- Decubitus ulcers: role of pressure and friction in causation [15]
- Etiologic factors in pressure sores: an experimental model [39]
- In vivo muscle stiffening under bone compression promotes deep pressure sore [40]
- Pressure ulcers: avoidable or unavoidable? Results of the National Pressure Ulcer Advisory Panel Consensus Conference [41]
- The decubitus ulcer: facts and controversies [42]
- Mechanical compression-indeced pressure sores in rat hindlimb: muscle stiffness, histology, and computational models [43]

2.2.2 Detection

- Combination of thermographic and ultrasonographic assessments for early detection of deep tissue injury [44]
- A review of deep tissue injury development, detection, and prevention [45]
- Pressure ulcer knowledge in medical residents: an opportunity for improvement [46]
- Clinical nurse' knowledge and visual differentiation ability in pressure ulcer classification system and incontinence-associated dermatitis [47]
- Toward real-time detection of deep tissue injury risk in wheelchair users using Hertz contact theory [48]
- Compression-induced deep tissue injury examined with magnetic resonance imaging and histology [49]

- Low-echoic lesions underneath the skin in subjects with spinal-cord injury [50]
- National Pressure Ulcer Advisory Panel's Updated Pressure Ulcer Staging System [31]
- A new pressure ulcer risk assessment scale for individuals with spinal cord injury [51]
- Deep tissue engineering from a bioengineering point of view [34]
- Evaluation of four non-invasive methods for examination and characterization of pressure ulcers [52]
- Which techniques to improve the early detection and prevention of pressure ulcers? [53]
- Inception and validation of a pressure ulcer risk scale in oncology [54]
- Assessment and management of pressure ulcers in the elderly: current strategies [8]
- Reliability testing of the national database of nursing quality indicators pressure ulcer indicator [55]
- Ultrasound assessment of deep tissue injury in pressure ulcers: possible prediction of pressure ulcer progression [56]
- 3D ultrasound elastography for early detection of lesions. Evaluation on a pressure ulcer mimicking phantom [57]

2.2.3 Prevention and Treatment

- Prevention of deep tissue injury through muscle contractions induced by intermittent electrical stimulation after spinal cord injury in pigs [58]

- The importance of internal strain as opposed to interface pressure in the prevention of pressure related deep tissue injury [37]

- New methodology for preventing pressure ulcers using actimetry and autonomous nervous system recording [59]

- Pressure ulcers: the great insult [9]

- Reaching for the moon: achieving zero pressure ulcer prevalence, an update [60]

- Distribution of Internal Pressure around Bony Prominences: Implications to deep tissue injury and effectiveness of intermittent electrical stimulation [35]

- Distribution of internal strains around bony prominences in pigs [36]

- Reaching for the moon: achieving zero pressure ulcer prevalence, an update. [60]

- Reducing pressure ulcers in hip fracture patients [61]

- Reducing pressure ulcer prevalence rates in the long-term acute care setting [10]

- Development of pressure ulcer program across a university health system [62]

- Assessment and management of pressure ulcers in the elderly: current strategies [8]

- Pressure ulcers: the great insult [9]

- Intermittent electrical stimulation redistributes pressure and promotes tissue oxygenation in loaded muscles of individuals with spinal cord injury. [63]

2.3 Ultrasound Elastography

Lorem ipsum dolor sit amet, consectetuer adipiscing elit. Ut purus elit, vestibulum ut, placerat ac, adipiscing vitae, felis. Curabitur dictum gravida mauris. Nam arcu libero, nonummy eget, consectetuer id, vulputate a, magna. Donec vehicula augue eu neque. Pellentesque habitant morbi tristique senectus et netus et malesuada fames ac turpis egestas. Mauris ut leo. Cras viverra metus rhoncus sem. Nulla et lectus vestibulum urna fringilla ultrices. Phasellus eu tellus sit amet tortor gravida placerat. Integer sapien est, iaculis in, pretium quis, viverra ac, nunc. Praesent eget sem vel leo ultrices bibendum. Aenean faucibus. Morbi dolor nulla, malesuada eu, pulvinar at, mollis ac, nulla. Curabitur auctor semper nulla. Donec varius orci eget risus. Duis nibh mi, congue eu, accumsan eleifend, sagittis quis, diam. Duis eget orci sit amet orci dignissim rutrum.

2.3.1 Quasi-Static Ultrasound Elastography

- A new method for the visualization and quantification of internal skin elasticity by ultrasound imaging [64]

2.3.2 Acoustic Radiation Force Impulse Imaging

- derp

2.3.3 Shear Wave Speed Quantification

- derp

2.4 Numerical Characterization / Finite-Element Modelling

Lorem ipsum dolor sit amet, consectetuer adipiscing elit. Ut purus elit, vestibulum ut, placerat ac, adipiscing vitae, felis. Curabitur dictum gravida mauris. Nam arcu libero, nonummy eget, consectetuer id, vulputate a, magna. Donec vehicula augue eu neque. Pellentesque habitant morbi tristique senectus et netus et malesuada fames ac turpis egestas. Mauris ut leo. Cras viverra metus rhoncus sem. Nulla et lectus vestibulum urna fringilla ultrices. Phasellus eu tellus sit amet tortor gravida placerat. Integer sapien est, iaculis in, pretium quis, viverra ac, nunc. Praesent eget sem vel leo ultrices bibendum. Aenean faucibus. Morbi dolor nulla, malesuada eu, pulvinar at, mollis ac, nulla. Curabitur auctor semper nulla. Donec varius orci eget risus. Duis nibh mi, congue eu, accumsan eleifend, sagittis quis, diam. Duis eget orci sit amet orci dignissim rutrum.

2.5 Conclusion

Lorem ipsum dolor sit amet, consectetuer adipiscing elit. Ut purus elit, vestibulum ut, placerat ac, adipiscing vitae, felis. Curabitur dictum gravida mauris. Nam arcu libero, nonummy eget, consectetuer id, vulputate a, magna. Donec vehicula augue eu neque. Pellentesque habitant morbi tristique senectus et netus et malesuada fames ac turpis egestas. Mauris ut leo. Cras viverra metus rhoncus sem. Nulla et lectus vestibulum urna fringilla ultrices. Phasellus eu

tellus sit amet tortor gravida placerat. Integer sapien est, iaculis in, pretium quis, viverra ac, nunc. Praesent eget sem vel leo ultrices bibendum. Aenean faucibus. Morbi dolor nulla, malesuada eu, pulvinar at, mollis ac, nulla. Curabitur auctor semper nulla. Donec varius orci eget risus. Duis nibh mi, congue eu, accumsan eleifend, sagittis quis, diam. Duis eget orci sit amet orci dignissim rutrum.

References

[1] J. Black, M. M. M. Baharestani, J. Cuddigan, B. Dorner, L. Edsberg, D. Langemo, M. E. E. Posthauer, C. Ratliff, G. Taler, and National Pressure Ulcer Advisory Panel, "National pressure ulcer advisory panel's updated pressure ulcer staging system.," *Advances in skin & wound care*, vol. 20, no. 5, pp. 269–274, May 2007, ISSN: 1527-7941. DOI: 10.1097/01.asw.0000269314.23015.e9. [Online]. Available: http://dx.doi.org/10.1097/01.asw.0000269314.23015.e9.

[2] L. Gunningberg and N. A. Stotts, "Tracking quality over time: what do pressure ulcer data show?" *International journal for quality in health care : journal of the International Society for Quality in Health Care / ISQua*, vol. 20, no. 4, pp. 246–253, Aug. 2008, ISSN: 1353-4505. DOI: 10.1093/intqhc/mzn009. [Online]. Available: http://dx.doi.org/10.1093/intqhc/mzn009.

[3] K. Beckrich and S. A. Aronovitch, "Hospital-acquired pressure ulcers: a comparison of costs in medical vs. surgical patients.," *Nursing economic$*, vol. 17, no. 5, pp. 263–271, 1999, ISSN: 0746-1739. [Online]. Available: http://view.ncbi.nlm.nih.gov/pubmed/10711175.

[4] J. M. Zanca, D. M. Brienza, D. Berlowitz, R. G. Bennett, C. H. Lyder, and National Pressure Ulcer Advisory Panel, "Pressure ulcer research funding in america: creation and analysis of an on-line database.," *Advances in skin & wound care*, vol. 16, no. 4, pp. 190–197, 2003, ISSN: 1527-7941. [Online]. Available: http://view.ncbi.nlm.nih.gov/pubmed/12897675.

[5] "Pressure ulcers in america: prevalence, incidence, and implications for the future. an executive summary of the national pressure ulcer advi-

sory panel monograph.," *Advances in skin & wound care*, vol. 14, no. 4, pp. 208–215, 2001, ISSN: 1527-7941. [Online]. Available: http://view.ncbi.nlm.nih.gov/pubmed/11902346.

[6] C. Russo, C. Steiner, and W. Spector, "Hospitalizations related to pressure ulcers among adults 18 years and older, 2006: statistical brief no. 64.," *Agency for Health Care Policy and Research (US)*, Dec. 2008. [Online]. Available: http://www.ncbi.nlm.nih.gov/sites/entrez?Db=pubmed%5C&%5C#38;Cmd=ShowDetailView%5C&%5C#38;TermToSearch=21595131.

[7] M. C. C. de Freitas, A. B. F. B. Medeiros, M. V. C. V. Guedes, P. C. C. de Almeida, F. T. T. de Galiza, and J. d. M. d. e. . M. Nogueira, "[pressure ulcers in the elderly: analysis of prevalence and risk factors].," *Revista gaúcha de enfermagem / EENFUFRGS*, vol. 32, no. 1, pp. 143–150, Mar. 2011, ISSN: 0102-6933. [Online]. Available: http://view.ncbi.nlm.nih.gov/pubmed/21888215.

[8] E. Jaul, "Assessment and management of pressure ulcers in the elderly: current strategies.," *Drugs & aging*, vol. 27, no. 4, pp. 311–325, Apr. 1, 2010, ISSN: 1170-229X. DOI: 10.2165/11318340-000000000-00000. [Online]. Available: http://dx.doi.org/10.2165/11318340-000000000-00000.

[9] J. Maklebust, "Pressure ulcers: the great insult.," *The Nursing clinics of North America*, vol. 40, no. 2, pp. 365–389, Jun. 2005, ISSN: 0029-6465. DOI: 10.1016/j.cnur.2004.09.015. [Online]. Available: http://dx.doi.org/10.1016/j.cnur.2004.09.015.

[10] C. T. Milne, D. Trigilia, T. L. Houle, S. Delong, and D. Rosenblum, "Reducing pressure ulcer prevalence rates in the long-term acute care

setting.," *Ostomy/wound management*, vol. 55, no. 4, pp. 50–59, Apr. 2009, ISSN: 0889-5899. [Online]. Available: http://view.ncbi.nlm.nih.gov/pubmed/19387096.

[11] A. Ingeman, G. Andersen, H. H. Hundborg, M. L. Svendsen, and S. P. Johnsen, "In-hospital medical complications, length of stay, and mortality among stroke unit patients.," *Stroke; a journal of cerebral circulation*, vol. 42, no. 11, pp. 3214–3218, Nov. 2011, ISSN: 1524-4628. DOI: 10.1161/strokeaha.110.610881. [Online]. Available: http://dx.doi.org/10.1161/strokeaha.110.610881.

[12] Z. B. Niazi, C. A. Salzberg, D. W. Byrne, and M. Viehbeck, "Recurrence of initial pressure ulcer in persons with spinal cord injuries.," *Advances in wound care : the journal for prevention and healing*, vol. 10, no. 3, pp. 38–42, 1997, ISSN: 1076-2191. [Online]. Available: http://view.ncbi.nlm.nih.gov/pubmed/9306777.

[13] A. Stekelenburg, D. Gawlitta, D. L. Bader, and C. W. Oomens, "Deep tissue injury: how deep is our understanding?" *Archives of physical medicine and rehabilitation*, vol. 89, no. 7, pp. 1410–1413, Jul. 2008, ISSN: 1532-821X. DOI: 10.1016/j.apmr.2008.01.012. [Online]. Available: http://dx.doi.org/10.1016/j.apmr.2008.01.012.

[14] J. A. Witkowski and L. C. Parish, "Histopathology of the decubitus ulcer.," *Journal of the American Academy of Dermatology*, vol. 6, no. 6, pp. 1014–1021, Jun. 1982, ISSN: 0190-9622. [Online]. Available: http://view.ncbi.nlm.nih.gov/pubmed/7096663.

[15] S. M. Dinsdale, "Decubitus ulcers: role of pressure and friction in causation.," *Archives of physical medicine and rehabilitation*, vol. 55, no.

4, pp. 147–152, Apr. 1974, ISSN: 0003-9993. [Online]. Available: http://view.ncbi.nlm.nih.gov/pubmed/4595834.

[16] R. Labbe, T. Lindsay, and P. M. Walker, "The extent and distribution of skeletal muscle necrosis after graded periods of complete ischemia.," *Journal of vascular surgery*, vol. 6, no. 2, pp. 152–157, Aug. 1987, ISSN: 0741-5214. DOI: 10.1067/mva.1987.avs0060152. [Online]. Available: http://dx.doi.org/10.1067/mva.1987.avs0060152.

[17] K. Ytrehus, O. Reikerås, N. Huseby, and R. Myklebust, "Ultrastructure of reperfused skeletal muscle: the effect of oxygen radical scavenger enzymes.," *International journal of microcirculation, clinical and experimental / sponsored by the European Society for Microcirculation*, vol. 15, no. 4, pp. 155–162, 1995, ISSN: 0167-6865. [Online]. Available: http://view.ncbi.nlm.nih.gov/pubmed/8847175.

[18] F. W. Blaisdell, "The pathophysiology of skeletal muscle ischemia and the reperfusion syndrome: a review.," *Cardiovascular surgery (London, England)*, vol. 10, no. 6, pp. 620–630, Dec. 2002, ISSN: 0967-2109. [Online]. Available: http://view.ncbi.nlm.nih.gov/pubmed/12453699.

[19] S. Tsuji, S. Ichioka, N. Sekiya, and T. Nakatsuka, "Analysis of ischemia-reperfusion injury in a microcirculatory model of pressure ulcers.," *Wound repair and regeneration*, vol. 13, no. 2, pp. 209–215, Mar. 2005, ISSN: 1067-1927. DOI: 10.1111/j.1067-1927.2005.130213.x. [Online]. Available: http://dx.doi.org/10.1111/j.1067-1927.2005.130213.x.

[20] K. K. Ceelen, A. Stekelenburg, S. Loerakker, G. J. Strijkers, D. L. Bader, K. Nicolay, F. P. Baaijens, and C. W. Oomens, "Compression-induced damage and internal tissue strains are related.," *Journal of biomechanics*, vol. 41, no. 16, pp. 3399–3404, Dec. 5, 2008, ISSN: 0021-9290. DOI: 10.

1016/j.jbiomech.2008.09.016. [Online]. Available: http://dx.doi.org/10.1016/j.jbiomech.2008.09.016.

[21] K. K. Ceelen, C. W. Oomens, and F. P. Baaijens, "Microstructural analysis of deformation-induced hypoxic damage in skeletal muscle.," *Biomechanics and modeling in mechanobiology*, vol. 7, no. 4, pp. 277–284, Aug. 2008, ISSN: 1617-7959. DOI: 10.1007/s10237-007-0097-7. [Online]. Available: http://dx.doi.org/10.1007/s10237-007-0097-7.

[22] S. Loerakker, L. R. Solis, D. L. Bader, F. P. Baaijens, V. K. Mushahwar, and C. W. Oomens, "How does muscle stiffness affect the internal deformations within the soft tissue layers of the buttocks under constant loading?" *Computer methods in biomechanics and biomedical engineering*, vol. 16, no. 5, pp. 520–529, 2013, ISSN: 1476-8259. DOI: 10.1080/10255842.2011.627682. [Online]. Available: http://dx.doi.org/10.1080/10255842.2011.627682.

[23] T. Nagel, S. Loerakker, and C. W. Oomens, "A theoretical model to study the effects of cellular stiffening on the damage evolution in deep tissue injury.," *Computer methods in biomechanics and biomedical engineering*, vol. 12, no. 5, pp. 585–597, Oct. 2009, ISSN: 1476-8259. DOI: 10.1080/10255840902788603. [Online]. Available: http://dx.doi.org/10.1080/10255840902788603.

[24] A. Gefen, "The biomechanics of sitting-acquired pressure ulcers in patients with spinal cord injury or lesions.," *International wound journal*, vol. 4, no. 3, pp. 222–231, Sep. 2007, ISSN: 1742-4801. DOI: 10.1111/j.1742-481x.2007.00330.x. [Online]. Available: http://dx.doi.org/10.1111/j.1742-481x.2007.00330.x.

[25] E. Linder-Ganz, N. Shabshin, Y. Itzchak, and A. Gefen, "Assessment of mechanical conditions in sub-dermal tissues during sitting: a combined experimental-MRI and finite element approach.," *Journal of biomechanics*, vol. 40, no. 7, pp. 1443–1454, 2007, ISSN: 0021-9290. DOI: 10.1016/j.jbiomech.2006.06.020. [Online]. Available: http://dx.doi.org/10.1016/j.jbiomech.2006.06.020.

[26] C. Then, J. Menger, T. J. Vogl, F. Hübner, and G. Silber, "Mechanical gluteal soft tissue material parameter validation under complex tissue loading.," *Technology and health care*, vol. 17, no. 5-6, pp. 393–401, 2009, ISSN: 1878-7401. DOI: 10.3233/thc-2009-0560. [Online]. Available: http://dx.doi.org/10.3233/thc-2009-0560.

[27] B. J. van Nierop, A. Stekelenburg, S. Loerakker, C. W. Oomens, D. Bader, G. J. Strijkers, and K. Nicolay, "Diffusion of water in skeletal muscle tissue is not influenced by compression in a rat model of deep tissue injury.," *Journal of biomechanics*, vol. 43, no. 3, pp. 570–575, Feb. 10, 2010, ISSN: 1873-2380. DOI: 10.1016/j.jbiomech.2009.07.043. [Online]. Available: http://dx.doi.org/10.1016/j.jbiomech.2009.07.043.

[28] R. M. Allman, P. S. Goode, M. M. Patrick, N. Burst, and A. A. Bartolucci, "Pressure ulcer risk factors among hospitalized patients with activity limitation.," *JAMA : the journal of the American Medical Association*, vol. 273, no. 11, pp. 865–870, Mar. 15, 1995, ISSN: 0098-7484. [Online]. Available: http://view.ncbi.nlm.nih.gov/pubmed/7869557.

[29] C. V. Bouten, C. W. Oomens, F. P. Baaijens, and D. L. Bader, "The etiology of pressure ulcers: skin deep or muscle bound?" *Archives of physical medicine and rehabilitation*, vol. 84, no. 4, pp. 616–619, Apr. 2003,

ISSN: 0003-9993. DOI: 10.1053/apmr.2003.50038. [Online]. Available: http://dx.doi.org/10.1053/apmr.2003.50038.

[30] R. Salcido, J. C. Donofrio, S. B. Fisher, E. K. LeGrand, K. Dickey, J. M. Carney, R. Schosser, and R. Liang, "Histopathology of pressure ulcers as a result of sequential computer-controlled pressure sessions in a fuzzy rat model.," *Advances in wound care : the journal for prevention and healing*, vol. 7, no. 5, Sep. 1994, ISSN: 1076-2191. [Online]. Available: http://view.ncbi.nlm.nih.gov/pubmed/7889250.

[31] J. Black, M. Baharestani, J. Cuddigan, B. Dorner, L. Edsberg, D. Langemo, M. E. E. Posthauer, C. Ratliff, G. Taler, and National Pressure Ulcer Advisory Panel, "National pressure ulcer advisory panel's updated pressure ulcer staging system.," *Dermatology nursing / Dermatology Nurses' Association*, vol. 19, no. 4, Aug. 2007, ISSN: 1060-3441. [Online]. Available: http://view.ncbi.nlm.nih.gov/pubmed/17874603.

[32] A. Gefen and E. Linder-Ganz, "[diffusion of ulcers in the diabetic foot is promoted by stiffening of plantar muscular tissue under excessive bone compression].," *Der Orthopäde*, vol. 33, no. 9, pp. 999–1012, Sep. 2004, ISSN: 0085-4530. DOI: 10.1007/s00132-004-0701-9. [Online]. Available: http://dx.doi.org/10.1007/s00132-004-0701-9.

[33] A. Gefen and E. Haberman, "Viscoelastic properties of ovine adipose tissue covering the gluteus muscles.," *Journal of biomechanical engineering*, vol. 129, no. 6, pp. 924–930, Dec. 2007, ISSN: 0148-0731. DOI: 10.1115/1.2800830. [Online]. Available: http://dx.doi.org/10.1115/1.2800830.

[34] A. Gefen, "Deep tissue injury from a bioengineering point of view.," *Ostomy/wound management*, vol. 55, no. 4, pp. 26–36, Apr. 2009, ISSN:

0889-5899. [Online]. Available: http://view.ncbi.nlm.nih.gov/pubmed/19387094.

[35] L. R. Solis, A. Liggins, R. R. Uwiera, N. Poppe, E. Pehowich, P. Seres, R. B. Thompson, and V. K. Mushahwar, "Distribution of internal pressure around bony prominences: implications to deep tissue injury and effectiveness of intermittent electrical stimulation.," *Annals of biomedical engineering*, pp. 1–20, Feb. 22, 2012, ISSN: 1521-6047. DOI: 10.1007/s10439-012-0529-0. [Online]. Available: http://dx.doi.org/10.1007/s10439-012-0529-0.

[36] L. R. Solis, A. B. Liggins, P. Seres, R. R. Uwiera, N. R. Poppe, E. Pehowich, R. B. Thompson, and V. K. Mushahwar, "Distribution of internal strains around bony prominences in pigs.," *Annals of biomedical engineering*, pp. 1–19, Mar. 8, 2012, ISSN: 1521-6047. DOI: 10.1007/s10439-012-0539-y. [Online]. Available: http://dx.doi.org/10.1007/s10439-012-0539-y.

[37] C. W. Oomens, S. Loerakker, and D. L. Bader, "The importance of internal strain as opposed to interface pressure in the prevention of pressure related deep tissue injury.," *Journal of tissue viability*, vol. 19, no. 2, pp. 35–42, May 2010, ISSN: 0965-206X. DOI: 10.1016/j.jtv.2009.11.002. [Online]. Available: http://dx.doi.org/10.1016/j.jtv.2009.11.002.

[38] E. Linder-Ganz and A. Gefen, "Stress analyses coupled with damage laws to determine biomechanical risk factors for deep tissue injury during sitting.," *Journal of biomechanical engineering*, vol. 131, no. 1, Jan. 2009, ISSN: 0148-0731. DOI: 10.1115/1.3005195. [Online]. Available: http://dx.doi.org/10.1115/1.3005195.

[39] R. K. Daniel, D. L. Priest, and D. C. Wheatley, "Etiologic factors in pressure sores: an experimental model.," *Archives of physical medicine and rehabilitation*, vol. 62, no. 10, pp. 492–498, Oct. 1981, ISSN: 0003-9993. [Online]. Available: http://view.ncbi.nlm.nih.gov/pubmed/7305643.

[40] A. Gefen, N. Gefen, E. Linder-Ganz, and S. S. Margulies, "In vivo muscle stiffening under bone compression promotes deep pressure sores.," *Journal of biomechanical engineering*, vol. 127, no. 3, pp. 512–524, Jun. 2005, ISSN: 0148-0731. [Online]. Available: http://view.ncbi.nlm.nih.gov/pubmed/16060358.

[41] J. M. Black, L. E. Edsberg, M. M. Baharestani, D. Langemo, M. Goldberg, L. McNichol, J. Cuddigan, and National Pressure Ulcer Advisory Panel, "Pressure ulcers: avoidable or unavoidable? results of the national pressure ulcer advisory panel consensus conference.," *Ostomy/wound management*, vol. 57, no. 2, pp. 24–37, Feb. 2011, ISSN: 1943-2720. [Online]. Available: http://view.ncbi.nlm.nih.gov/pubmed/21350270.

[42] C. Campbell and L. C. C. Parish, "The decubitus ulcer: facts and controversies.," *Clinics in dermatology*, vol. 28, no. 5, pp. 527–532, Sep. 2010, ISSN: 1879-1131. DOI: 10.1016/j.clindermatol.2010.03.010. [Online]. Available: http://dx.doi.org/10.1016/j.clindermatol.2010.03.010.

[43] E. Linder-Ganz and A. Gefen, "Mechanical compression-induced pressure sores in rat hindlimb: muscle stiffness, histology, and computational models.," *Journal of applied physiology (Bethesda, Md. : 1985)*, vol. 96, no. 6, pp. 2034–2049, Jun. 2004, ISSN: 8750-7587. DOI: 10.1152/

japplphysiol.00888.2003. [Online]. Available: http://dx.doi.org/10.1152/japplphysiol.00888.2003.

[44] T. Higashino, G. Nakagami, T. Kadono, Y. Ogawa, S. Iizaka, H. Koyanagi, S. Sasaki, N. Haga, and H. Sanada, "Combination of thermographic and ultrasonographic assessments for early detection of deep tissue injury.," *International wound journal*, Nov. 22, 2012, ISSN: 1742-481X. DOI: 10.1111/j.1742-481x.2012.01117.x. [Online]. Available: http://dx.doi.org/10.1111/j.1742-481x.2012.01117.x.

[45] A. Gefen, K. J. Farid, and I. Shaywitz, "A review of deep tissue injury development, detection, and prevention: shear savvy.," *Ostomy/wound management*, vol. 59, no. 2, pp. 26–35, Feb. 2013, ISSN: 1943-2720. [Online]. Available: http://view.ncbi.nlm.nih.gov/pubmed/23388395.

[46] J. M. Levine, E. A. Ayello, K. M. Zulkowski, and J. Fogel, "Pressure ulcer knowledge in medical residents: an opportunity for improvement.," *Advances in skin & wound care*, vol. 25, no. 3, pp. 115–117, Mar. 2012, ISSN: 1538-8654. DOI: 10.1097/01.asw.0000412908.43335.46. [Online]. Available: http://dx.doi.org/10.1097/01.asw.0000412908.43335.46.

[47] Y. J. J. Lee, S. Park, J. Y. Y. Kim, C. G. G. Kim, and S. K. K. Cha, "[clinical nurses' knowledge and visual differentiation ability in pressure ulcer classification system and incontinence-associated dermatitis].," *Journal of Korean Academy of Nursing*, vol. 43, no. 4, pp. 526–535, Aug. 2013, ISSN: 2093-758X. DOI: 10.4040/jkan.2013.43.4.526. [Online]. Available: http://dx.doi.org/10.4040/jkan.2013.43.4.526.

[48] L. Agam and A. Gefen, "Toward real-time detection of deep tissue injury risk in wheelchair users using hertz contact theory.," *Journal of*

rehabilitation research and development, vol. 45, no. 4, 2008, ISSN: 1938-1352. [Online]. Available: http://view.ncbi.nlm.nih.gov/pubmed/18712639.

[49] A. Stekelenburg, C. W. Oomens, G. J. Strijkers, K. Nicolay, and D. L. Bader, "Compression-induced deep tissue injury examined with magnetic resonance imaging and histology.," *Journal of applied physiology (Bethesda, Md. : 1985)*, vol. 100, no. 6, pp. 1946–1954, Jun. 2006, ISSN: 8750-7587. DOI: 10.1152/japplphysiol.00889.2005. [Online]. Available: http://dx.doi.org/10.1152/japplphysiol.00889.2005.

[50] N. Kanno, T. Nakamura, M. Yamanaka, K. Kouda, T. Nakamura, and F. Tajima, "Low-echoic lesions underneath the skin in subjects with spinal-cord injury.," *Spinal cord*, vol. 47, no. 3, pp. 225–229, Mar. 2009, ISSN: 1362-4393. DOI: 10.1038/sc.2008.101. [Online]. Available: http://dx.doi.org/10.1038/sc.2008.101.

[51] C. A. Salzberg, D. W. Byrne, C. G. Cayten, P. van Niewerburgh, J. G. Murphy, and M. Viehbeck, "A new pressure ulcer risk assessment scale for individuals with spinal cord injury.," *American journal of physical medicine & rehabilitation / Association of Academic Physiatrists*, vol. 75, no. 2, pp. 96–104, 1996, ISSN: 0894-9115. [Online]. Available: http://view.ncbi.nlm.nih.gov/pubmed/8630201.

[52] E. Sloth and T. Karlsmark, "Evaluation of four non-invasive methods for examination and characterization of pressure ulcers.," *Skin research and technology : official journal of International Society for Bioengineering and the Skin (ISBS) [and] International Society for Digital Imaging of Skin (ISDIS) [and] International Society for Skin Imaging (ISSI)*, vol. 14, no. 3, pp. 270–276, Aug. 2008, ISSN: 1600-0846. DOI: 10.1111/j.1600-

0846.2008.00290.x. [Online]. Available: http://dx.doi.org/10.1111/j.1600-0846.2008.00290.x.

[53] C. Gehin, E. Brusseau, R. Meffre, P. M. Schmitt, J. F. Deprez, and A. Dittmar, "Which techniques to improve the early detection and prevention of pressure ulcers?" *Conference proceedings : ... Annual International Conference of the IEEE Engineering in Medicine and Biology Society. IEEE Engineering in Medicine and Biology Society. Conference*, vol. 1, pp. 6057–6060, 2006, ISSN: 1557-170X. DOI: 10.1109/iembs.2006.259506. [Online]. Available: http://dx.doi.org/10.1109/iembs.2006.259506.

[54] I. Fromantin, M. C. Falcou, A. Baffie, C. Petot, R. Mazerat, C. Jaouen, L. Téot, and d. Rycke, "Inception and validation of a pressure ulcer risk scale in oncology.," *Journal of wound care*, vol. 20, no. 7, Jul. 2011, ISSN: 0969-0700. [Online]. Available: http://view.ncbi.nlm.nih.gov/pubmed/21841721.

[55] S. Hart, S. Bergquist, B. Gajewski, and N. Dunton, "Reliability testing of the national database of nursing quality indicators pressure ulcer indicator.," *The Journal of nursing administration*, vol. 40, no. 10 Suppl, Oct. 2010, ISSN: 1539-0721. DOI: 10.1097/nna.0b013e3181f37d15. [Online]. Available: http://dx.doi.org/10.1097/nna.0b013e3181f37d15.

[56] N. Aoi, K. Yoshimura, T. Kadono, G. Nakagami, S. Iizuka, T. Higashino, J. Araki, I. Koshima, and H. Sanada, "Ultrasound assessment of deep tissue injury in pressure ulcers: possible prediction of pressure ulcer progression.," *Plastic and reconstructive surgery*, vol. 124, no. 2, pp. 540–550, Aug. 2009, ISSN: 1529-4242. DOI: 10.1097/prs.0b013e3181addb33. [Online]. Available: http://dx.doi.org/10.1097/prs.0b013e3181addb33.

[57] J.-F. F. Deprez, G. Cloutier, C. Schmitt, C. Gehin, A. Dittmar, O. Basset, and E. Brusseau, "3D ultrasound elastography for early detection of lesions. evaluation on a pressure ulcer mimicking phantom.," *Conference proceedings : ... Annual International Conference of the IEEE Engineering in Medicine and Biology Society. IEEE Engineering in Medicine and Biology Society. Conference*, vol. 2007, pp. 79–82, 2007, ISSN: 1557-170X. DOI: 10.1109/iembs.2007.4352227. [Online]. Available: http://dx.doi.org/10.1109/iembs.2007.4352227.

[58] L. R. Solis, E. Twist, P. Seres, R. B. Thompson, and V. K. Mushahwar, "Prevention of deep tissue injury through muscle contractions induced by intermittent electrical stimulation after spinal cord injury in pigs.," *Journal of applied physiology (Bethesda, Md. : 1985)*, vol. 114, no. 2, pp. 286–296, Jan. 15, 2013, ISSN: 1522-1601. DOI: 10.1152/japplphysiol.00257.2012. [Online]. Available: http://dx.doi.org/10.1152/japplphysiol.00257.2012.

[59] R. Meffre, C. Gehin, P. M. Schmitt, F. De Oliveira, and A. Dittmar, "New methodology for preventing pressure ulcers using actimetry and autonomous nervous system recording.," *Conference proceedings : ... Annual International Conference of the IEEE Engineering in Medicine and Biology Society. IEEE Engineering in Medicine and Biology Society. Conference*, vol. 1, pp. 5563–5566, 2006, ISSN: 1557-170X. DOI: 10.1109/iembs.2006.259352. [Online]. Available: http://dx.doi.org/10.1109/iembs.2006.259352.

[60] I. Bales and T. Duvendack, "Reaching for the moon: achieving zero pressure ulcer prevalence, an update.," *Journal of wound care*, vol. 20, no. 8, Aug. 2011, ISSN: 0969-0700. [Online]. Available: http://view.ncbi.nlm.nih.gov/pubmed/21841712.

[61] M. Thompson, "Reducing pressure ulcers in hip fracture patients.," *British journal of nursing (Mark Allen Publishing)*, vol. 20, no. 15, 2011, ISSN: 0966-0461. [Online]. Available: http://view.ncbi.nlm.nih.gov/pubmed/21841645.

[62] D. Carson, K. Emmons, W. Falone, and A. M. M. Preston, "Development of pressure ulcer program across a university health system.," *Journal of nursing care quality*, Sep. 10, 2011, ISSN: 1550-5065. DOI: 10.1097/ncq.0b013e3182310f8b. [Online]. Available: http://dx.doi.org/10.1097/ncq.0b013e3182310f8b.

[63] S. Gyawali, L. Solis, S. L. L. Chong, C. Curtis, P. Seres, I. Kornelsen, R. Thompson, and V. K. Mushahwar, "Intermittent electrical stimulation redistributes pressure and promotes tissue oxygenation in loaded muscles of individuals with spinal cord injury.," *Journal of applied physiology (Bethesda, Md. : 1985)*, vol. 110, no. 1, pp. 246–255, Jan. 2011, ISSN: 1522-1601. DOI: 10.1152/japplphysiol.00661.2010. [Online]. Available: http://dx.doi.org/10.1152/japplphysiol.00661.2010.

[64] O. Osanai, M. Ohtsuka, M. Hotta, T. Kitaharai, and Y. Takema, "A new method for the visualization and quantification of internal skin elasticity by ultrasound imaging.," *Skin research and technology : official journal of International Society for Bioengineering and the Skin (ISBS) [and] International Society for Digital Imaging of Skin (ISDIS) [and] International Society for Skin Imaging (ISSI)*, Feb. 23, 2011, ISSN: 1600-0846. DOI: 10.1111/j.1600-0846.2010.00492.x. [Online]. Available: http://dx.doi.org/10.1111/j.1600-0846.2010.00492.x.

Chapter 3

Numerical Characterization of Quasi-Static Ultrasound Elastography

3.1 Introduction

The goal of this study was to numerically characterize various important parameters related to detecting DTI using quasi-static ultrasound elastography (such as lesion geometry, material properties, and transducer characteristics) in order to examine the feasibility of using the technique to detect early DTI in humans. Quasi-static ultrasound elastography involves displacing the surface of the skin such that internal tissues are placed under a strain field. Ultrasound signals are used to track internal strains which then relate to the localized mechanical stiffness of the tissue — local regions that are significantly more or less stiff than surrounding tissue may be classified as either undergoing rigor mortis or necrosis and may present cause for concern.

3.2 Method

In order to evaluate the sensitivity of using quasi-static ultrasound elastography to detect deep tissue injuries, a numerical model of these injuries was created such that a subset of the investigated cases mimicked a physical phantom model which was used for validation. This numerical model allowed the rapid modification of numerous parameters related to DTI to examine their effect on the method's detection sensitivity where detection sensitivity is defined as the slope of the given characterization plot[c1]. To fully understand the problem, 5 general model cases [c2] were studied with each case [c3]generating numerous sub-studies on the effect of various parameters relating to that case. These parameters included: lesion depth; lesion altitude (distance of the lesion above deep bone); lesion diameter; ratio of the stiffness between the lesion and the surrounding tissue; ultrasound probing frequency; strain level applied by the transducer; the separation distance between two co-located lesions; radius of a circular averaging filter applied to the lesion boundaries; the number of smaller clustered lesions per unit area; the radius of each individual clustered lesion; the width of the lesion in a Visible Human [1] model and the depth of the lesion in a Visible Human model. The range of values for the tested parameters are given in Table 3.1 which resulted in a total of 144 model cases that were analyzed[c4]. The geometry of the models shown in Fig. 3.1 include: a simple spherical lesion embedded within a 2-dimensional rectangular zone of soft tissue; two lesions located at the same depth separated laterally by a finite dimension, δ_{sep}; a spherical lesion without hard boundaries; a cluster of small lesions which together form a larger lesion area; and a lesion with mri-acquired

[c1] *KH*: Added definition for detection sensitivity

[c2] *KH*: Added models to study co-located lesions, lesions with blurred boundaries, clusters of small lesions, and a lesion in a human tissue domain

[c3] *MFP*: ~~investigating~~

[c4] *KH*: Increased number of investigated models for 64 to 144

Table 3.1: Range of values of investigated parameters

Parameter	Symbol	Values
Lesion depth	d	$[3.5, 6.5, 8.5, 10.0]$ cm
Lesion altitude	h	$[1.25, 2.50, 3.75]$ cm
Lesion diameter	$\varnothing S$	$[0.5, 1.0, 2.0, 2.5]$ cm
Lesion stiffness ratio	E_{rel}	$[0.32, 0.56, 1.80, 3.20]$
Ultrasound frequency	f	$[2, 4, 8]$ MHz
Transudcer-applied strain	ε_{app}	$[2.5, 5.0, 10.0]$ %
Colocated separation distance	δ_{sep}	$[1.25, 1.50, 1.75, 2.00]$ cm
Blurred lesion blur radius	b_r	$[1.0, 2.5, 5.0, 7.5]$ mm
Clustered lesion density	b_ρ	$[10, 20, 30, 40]$ cm^{-2}
Clustered lesion radius	r_{bl}	$[0.5, 1.0, 1.5]$ mm
Visible human lesion width	$\varnothing S$	$[0.5, 1.0, 2.0, 2.5]$ cm
Visible human lesion depth	d	$[6.25, 6.75, 7.25]$ cm

geometry [2] embedded in geometry obtained from a Visible Human slice [1].

In Fig. 3.1e, the lesion is located superficial to the left ischial tuberosity in the transverse plane. The lesion geometry was obtained from an MRI scan of a real deep tissue injury induced in a porcine model [2]. The generic soft tissue in this model is modelled after muscle, with a layer of adipose tissue residing at the surface of the model.

Note that the axial direction referred to henceforth [c1]as the "axial" direction of an ultrasound transducer placed along the top (superficial) surface of the domain such that it becomes the "vertical" direction.

Simulated ultrasound images were acquired through the convolution of a point spread function with a normally distributed background map of scattering centres [3]. These images were then combined with a finite-element deformation model of the strained tissue to generate both pre- and post- compression images of the lesions and surrounding tissue. These images were fed into a tissue strain estimation algorithm to determine the detection sensitivity of the technique. Finally, the technique was validated against a physical

[c1] *MFP*: ~~represents~~

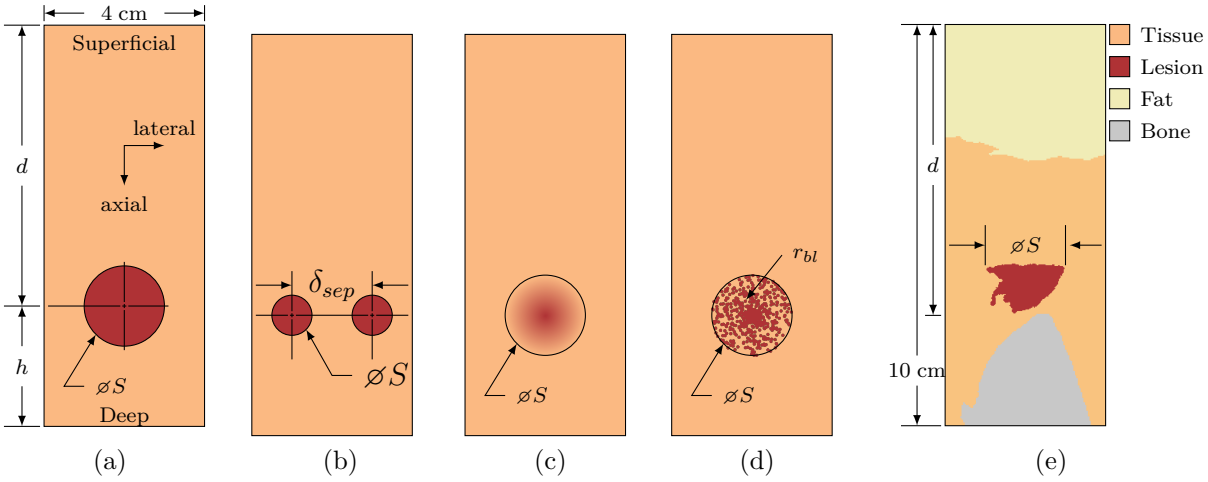

Figure 3.1: Model geometry showing the investigated lesions embedded in a 4 cm wide soft tissue domain. Axial and lateral directions mimic that of a typical ultrasound transducer placed along the top boundary of the domain. The simplest case of a circular lesion embedded in a soft tissue domain located superior to hard underlying bone is shown in (a). In order to investigate the interference caused by closely-located lesions, the case shown in (b) was investigated. Because of the relatively unknown and variable geometric properties of deep tissue injury lesions, cases (c) and (d) were investigated where the lesion edges were blurred and the lesion was actually a large collection of small lesions, respectively. Finally, to investigate detection sensitivity in a realistic setting, case (e) was investigated where an mri-acquired deep tissue injury was overlaid on a slice from the Visible Human Project such that the injury lesion was located immediately superior to an ischial tuberosity.

phantom model using a subset of the simulated cases.

3.2.1 Formation of B-Mode Ultrasound Images

[c1] Through the convolution of a point spread function and a normal random distribution of scattering centres, simulated ultrasound images were generated. The point spread function was defined axially as a cosine function operating at the ultrasound probing frequency modulated by a Gaussian distribution defined by $\mu = 2\lambda$ and $\sigma = 2\lambda$ where λ is the wavelength of the ultrasonic probing waves. Laterally, the point spread function was modelled as a Gaus-

[c1] *KH*: The method of ultrasound simulation has been changed from a pure acoustic simulation to the one recommended by reviewer 3

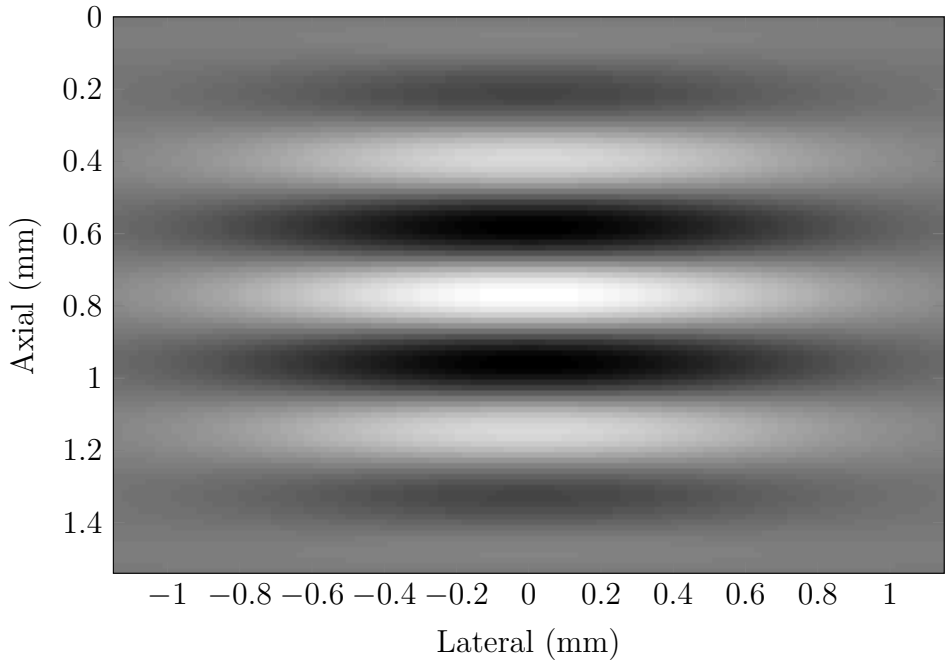

Figure 3.2: Point spread function used for simulating b-mode ultrasound scans. The function is defined axially by a cosine function at the probing frequency and modulated by a Gaussian function both axially and laterally.

sian distribution defined by $\mu = 0$ and $\sigma = 0.25 w_{active}$ where w_{active} is the total width of the active transducer elements during scan-line acquisition. This resulted in the point spread function given in Fig. 3.2. Resulting images were composed of 192 scan lines each sampled at 50 MHz.

3.2.2 Finite-Element Model of Tissue Deformation Under Surface Distortion

As a response to an external load being applied to the boundary of a domain, internal structures deform. In the case of a relatively stiff deep tissue injury embedded within surrounding soft tissues, this implies that when the surface of the skin is depressed, the relatively stiff lesion will not strain to the same magnitude that the surrounding soft tissue does. In order to simulate the deformation of interrogated tissue, the displacement field for the simulated

models was calculated according to:

$$-\nabla \cdot \sigma = F \tag{3.1}$$

Where σ is the Cauchy stress tensor and F are the applied body forces[c1]. Simulations were performed assuming a 2-dimensional linearly elastic material deformation model under plane strain conditions. A 3-dimensional model was also considered, however the deformations differed from the 2-dimensional simulation by less than 1 % so a 2-dimensional model was deemed adequate[c2]. Soft tissue was modelled using a Young's modulus of elasticity of 25 kPa, Poisson's ratio of 0.499, and density of 998 kg/m^3 [4]–[6]. The only difference in lesion mechanical properties from the surrounding soft tissue was the modulus of elasticity which varied according to the simulation parameters. The bottom of the domain was held fixed such that:

$$u = 0, \qquad \Gamma = \Gamma_{bottom} \tag{3.2}$$

While this boundary condition represents an idealized scenario, it may be likened to that of tissue located superficial to a relatively stiff anchoring bone below. This lower region is where deep tissue injuries generally form and is therefore of special importance. Compressive strains were applied to the top of the domain so as to induce strain along the top boundary:

$$u = (0, -u_0), \qquad \Gamma = \Gamma_{top} \tag{3.3}$$

From these simulations, displacement fields throughout the domain were calculated which were then used to displace tissue (including scattering cen-

[c1] *KH*: fixed typo from "tractions" to "body forces"
[c2] *KH*: included reasoning for 2D model over 3D

tres) in the simulated ultrasound images in both the axial and lateral directions. This process resulted in pairs of pre- and post- compression simulated b-mode images of lesions of varying parameters which could then be analyzed and characterized.

3.2.3 Characterizing Quasi-Static Ultrasound Elastography

Utilizing a 2-[c1]D locally regularized tissue strain estimation algorithm [7], pairs of pre- and post- compression images were used to calculate elastogram estimations for the full range of parameter values of the simulated lesions. The algorithm consists of sweeping the image domain with a series of overlapping regions of interest (ROI). ROI are compared between pre- and post- compression images, with ROI in the post- compression images being axially scaled and translated and laterally translated versions of the same ROI in the pre-compression images.

Qualitatively, the noise and computation time of the resulting elastograms were[c2] found to be minimum when using an axial ROI size of approximately 10 times the ultrasound wavelength. Axial ROI overlap was held at 99 % to produce elastograms with minimal noise, even though this introduced significant increases in computation time. Due to the extreme anisotropic nature of ultrasound signals, lateral ROI size was kept to 5 signal widths with lateral ROI overlaps of 80 %.

[c1] *MFP*: ~~d~~

[c2] *KH*: corrected typo "was" to "were"

Table 3.2: CIRS Phantom Model Mechanical Properties

Property	Value
[c1]Nominal basal stiffness	25 kPa
Lesion stiffness	$[8, 14, 45, 80]$ kPa
Speed of sound	1540 m/s
Acoustic attenuation	0.5 dB/cm MHz
Lesion diameter	$[10, 20]$ mm
Lesion depth	$[15, 35]$ mm

3.2.4 Model Validation Using a Commercially Available Phantom

Utilizing a CIRS Elasticity QA Phantom model 049, a subset of the results obtained from the finite-element simulations and numerical characterizations were compared against their physical phantom equivalents. The phantom mimics acoustically homogeneous soft tissue with embedded lesions which vary in depth, size, and mechanical stiffness. Mechanical properties of the phantom as given by manufacturer specifications are summarized in Table 3.2. Pre- and post- compression b-mode ultrasound images were obtained of each lesion in the phantom and the resulting strain ratio for that lesion was compared to the simulated strain ratio for that combination of parameters. Specifically, lesions at a depth of 3.5 cm, a diameter of 2.0 cm, and with true stiffness ratios of 0.56, 1.80, and 3.20 were examined. Surface indentation was performed manually with the transducer indenting approximately 0.5 cm (6.25 %) at the surface. [c3]

[c3] *KH*: New experiments were performed

3.3 Results

[c2]Following the procedure outlined in Section 3.2, finite-element models of ultrasonic b-mode image formation and tissue deformation were synthesized. The results of these models were then fed into the local strain estimation algorithm described in Section 3.2.3. The resulting numerical characterizations of the relationship between measured and true strain ratios in the simulated tissue and their dependence on the various lesion parameters given in Table 3.1 were examined. Finally, the local strain estimation algorithm was carried out on a physical phantom and compared against a subset of the simulated cases.

3.3.1 Finite Element Models of Ultrasound and Deformation

Sample images generated using both the acoustic and deformation finite-element models are given in Figs. 3.3a, 3.3b and 3.3c. In Fig. 3.3a, a sample generated b-mode ultrasound scan is given. Fig. 3.3b shows the vector-sum displacement field generated by the deformation finite-element model. The entire top surface of the model has been displaced axially by 6.25 mm (5 %), which caused deformation of both the soft tissue and embedded lesion within. Since the lesion was modelled as being 3.2 times stiffer than the surrounding tissue, the lesion underwent less strain which consequently resulted in the lesser displacement depicted. Fig. 3.3c shows the resultant b-mode image generated by applying the displacement field given in Fig. 3.3b to the tissue and embedded scattering centres used to create Fig. 3.3a. What results is a locally scaled and translated version of Fig. 3.3a that corresponds to indent-

[c2] *KH*: Completely new results section due to the new b-mode image formation technique and inclusion of new models.

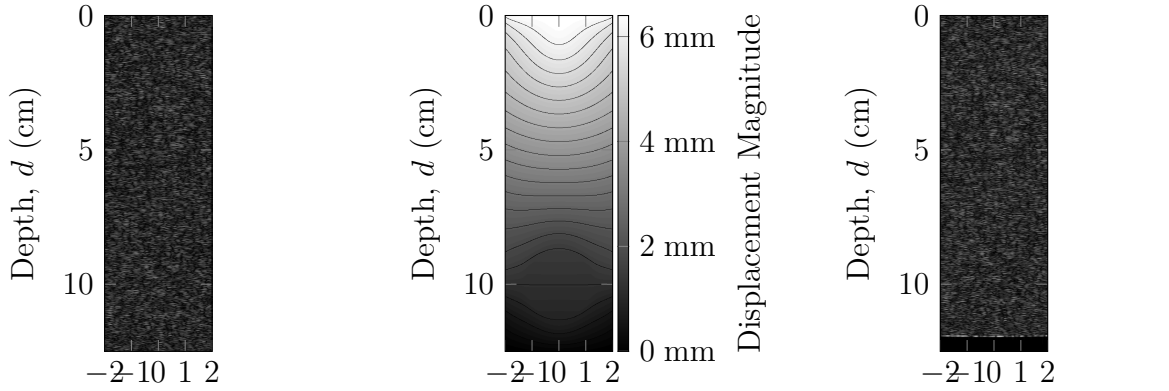

Figure 3.3: Finite-element model results for the case when $d = 10$ cm, $\varnothing S = 2.5$ cm, $\varepsilon_{rel} = 3.20$, and $f = 4$ MHz showing (a) a generated b-mode image of the pre-compressed tissue domain, (b) the vector-summed displacement field induced by compressive strain applied to the top of the boundary, and (c) a generated b-mode image of the post-compressed tissue domain. The included lesion is not visible in (a) and (c) as it's acoustic properties were no different than surrounding tissues. An anechoic region is visible along the bottom of the domain in (c) which represents tissue outside of the domain visible in (a).

ing the surface of the skin above a stiff lesion. The large [c1]anechoic region located at the bottom of the domain is tissue that was not modelled in the pre-compression image as it was outside of the original domain. This area represents the region of tissue that is undetectable with the strain-estimation algorithm given in Section 3.2.3 as the information contained there is only available in one of the two input images and so is considered incomplete data.

3.3.2 Resulting Elastograms

The 2-[c1]D locally regularized tissue strain estimation algorithm described in Section 3.2.3 was used in combination with the simulated resultant b-mode ultrasound images (Figs. 3.3a and 3.3c) in order to generate elastogram images

[c1] *MFP*: ~~hypoechoic~~
[c1] *MFP*: ~~d~~

which were used in the subsequent analysis. An example elastogram resulting from the simulation presented in Fig. 3.3 is shown in Fig. 3.4. Throughout the entire domain on this sample elastogram, regions outside of the stiff lesions showed compressive strains of approximately 5 % as expected due to the compression applied to the upper boundary of the model. The entire lesion region showed relatively consistent low strain amounts of approximately 2.5 %, which is consistent with the lesion being stiffer (and so straining less) than the surrounding tissue. Of [c2]note is the increased strain pattern which appeared both axially and laterally around the lesion. While generally symmetric about the axial direction, this stress field was largely concentrated above the lesion when the lesion was deep (close to the bone). This may be explained as a stress concentration brought about by the sudden change in mechanical material properties of the tissue and may serve to fuel the conditions of excessive cell deformation and ischemia which initiated the formation of a deep tissue injury in the first place, exacerbating the wound and assisting its expansion toward the surface.

3.3.3 Numerical Characterizations

In order to determine the sensitivity of using quasi-static ultrasound elastography to detect deep tissue injuries, elastograms such as the example that was calculated in Section 3.3.2 were calculated for the full range of parameters given in Table 3.1. "Measured" strain ratios for each elastogram were obtained by comparing the mean strain within each lesion with the mean [c1]engineering strain of the surrounding tissue such that:

$$\varepsilon_{rel,measured} = \frac{\varepsilon_{tissue}}{\varepsilon_{lesion}} \tag{3.4}$$

[c2] *MFP*: ~~interest to~~
[c1] *MFP*: *Text added.*

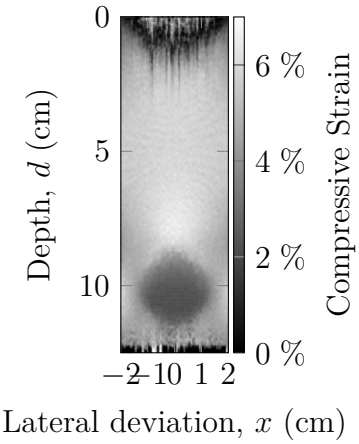

Figure 3.4: Sample strain elastogram showing estimated strain values for $d = 10$ cm, $\varnothing S = 2.5$ cm, $\varepsilon_{rel} = 3.20$, $f = 4$ MHz. While undetectable on a single b-mode image, the elastogram clearly shows a low-strain (stiff) lesion located approximately 10 cm from the surface.

ε_{tissue} was sampled as the mean strain in the region of tissue with the same geometry as the lesion located immediately superficial to the lesion in all cases.

In order to characterize how each parameter of interest affects the detection sensitivity of quasi-static ultrasound elastography, measured strain ratios for various lesions were calculated and compared against $\varepsilon_{rel,true}$. $\varepsilon_{rel,true}$ is derived from the relative Young's modulus of elasticity of the lesion such that:[c1]

$$\varepsilon_{rel,true} = \frac{\varepsilon_{tissue}}{\varepsilon_{lesion}} = \frac{\left(\frac{\sigma_{applied}}{E_{tissue}}\right)}{\left(\frac{\sigma_{applied}}{E_{lesion}}\right)} = \frac{E_{lesion}}{E_{tissue}} \tag{3.5}$$

Fig. 3.5 portrays the severe error involved with using the methods described in Section 3.2 to investigate extremely [c2]low stiffness lesions. In nearly all investigated cases where the true lesion stiffness ratio was 0.32, the algorithms described severely misrepresented the measured strain ratio of the lesion, often portraying these extremely [c3]low stiffness regions as being more stiff than they truly were. It is hypothesized that the excessively large localized

[c1] *MFP*: Add quick derivation
[c2] *MFP*: ~~soft (mushy)~~
[c3] *MFP*: ~~soft~~

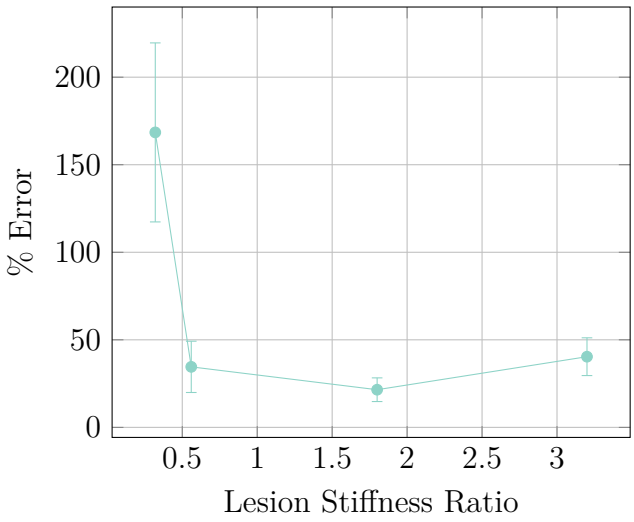

Figure 3.5: Detection ability as it related to true lesion stiffness ratio. For all but small lesion stiffness ratios (very soft "lesions"), results are linear and predictable. For small lesion stiffness ratios (0.32), the lesion becomes severely misrepresented. This is likely due to the algorithm "losing track" of scattering centers for the relatively large displacements induced in the signiciantly less stiff tissue.

deformations in these lesions interrupted the algorithm's ability to sufficiently track the displacement of scattering centres within the tissue, lowering the magnitude of displacement within the lesion and subsequently increasing it's "measured" strain ratio.

In order to broadly investigate the critical parameter-values of the investigated models, each parameter was normalized to it's investigated range and the error resulting over these ranges is given in Figs. 3.6 and 3.7.

In Fig. 3.6, it is clear to see that the most sensitive error-inducing situations occur when either the lesion is very small or if large strains are used to deform the tissue. Similarly, it is expected that if the lesion depth were increased much further, significant errors would arise with increasing depth. Logically, this may be explained due to the decreasing magnitude of displacement with increasing depth — at a certain point, the magnitude of displacement of scattering centres will be on par with the measurement noise, and the lesion will

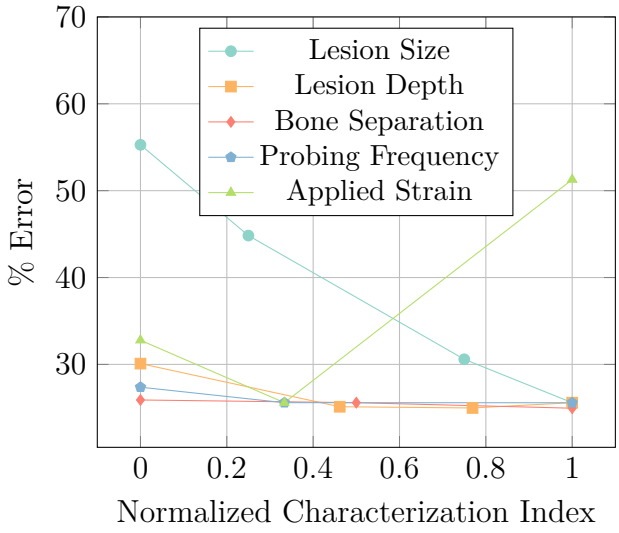

Figure 3.6: Error characterization for range of studied parameters for the simple model of a spherical lesion embedded within soft tissue as seen in Fig. 3.1a. Each parameter has been normalized to the range studied so overly-sensitive regions may be readily distinguished.

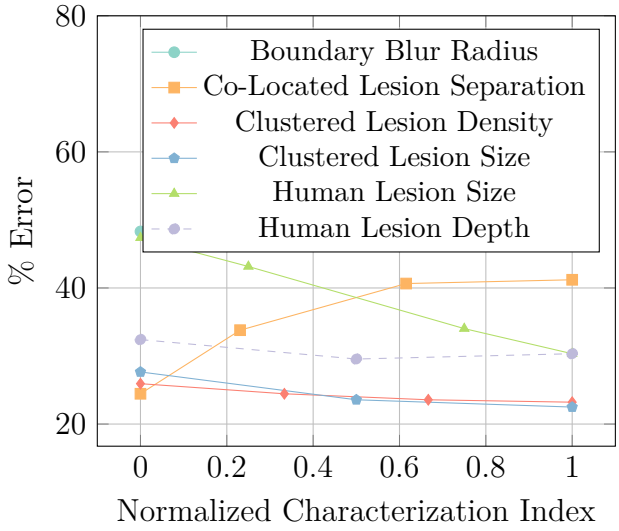

Figure 3.7: Error characterization for range of studied parameters for the co-located lesions, blurred boundary lesions, clustered lesions, and visible human lesion models as seen in Figs. 3.1b – 3.1e. Each parameter has been normalized to the range studied so overly-sensitive regions may be readily distinguished.

cease to be detectable.

From Fig. 3.7 it can be seen that small lesions in the Visible Human-MRI model as well as co-located lesions with large separation distances produce

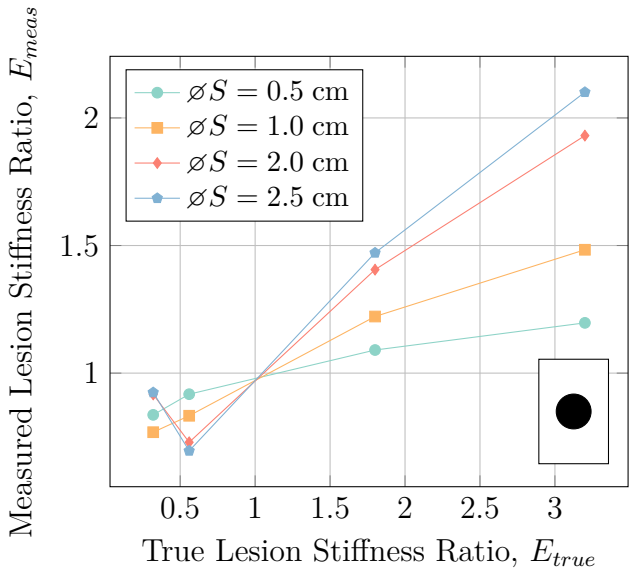

Figure 3.8: Lesion size characterization at a depth of 10 cm with a 4 MHz ultrasound probing frequency showing increasing detection sensitivity of the lesion with increasing lesion size. Detection sensitivity is less than ideal for all cases, with the best case being for lesions approximately 2.5 cm in diameter.

greater measurement errors. Conversely, lesion depth in the Visible Human-MRI model; lesion density and individual lesion size in the clustered lesion model; and boundary blur radius in the blurred-edges model do not seem to affect the measurement error significantly. Of note is the relative large amount of static error present in the boundary blur radius model which is hypothesized to be due to lesser mean tissue stiffness in the investigated region than expected.

Fig. 3.8 shows the relationship between lesion size and detection sensitivity for lesions at a depth of 10 cm in a model depth of 12.5 cm interrogated at 4 MHz with 5 % applied strain. Specifically, Fig. 3.8 shows the decreasing detection sensitivity with decreasing lesion size with the best detection sensitivity being with the largest investigated lesions with a diameter of 2.5 cm. On the opposite end, the detection sensitivity of lesions at or below 0.5 cm in diameter is questionable. This level of detection ability (with regards to lesion

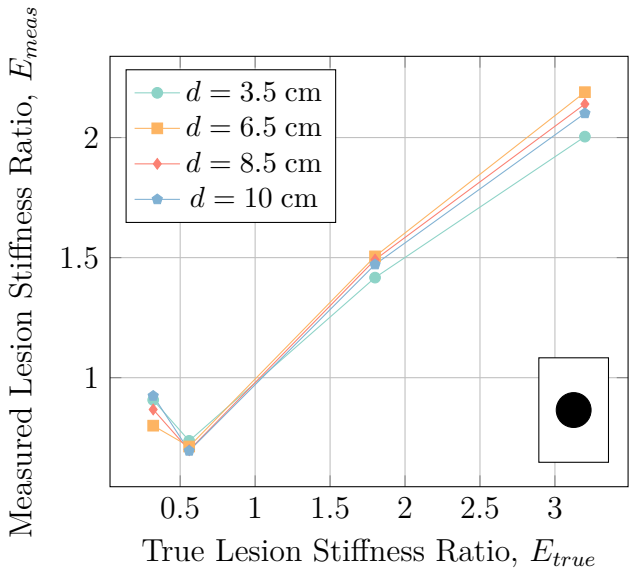

Figure 3.9: Lesion depth characterization at a lesion diameter of 2.5 cm with a 4 MHz ultrasound probing frequency generally showing general independence of detection sensitivity on lesion depth in the tissue.

size) is acceptable, however, as although there is little data on the true size of formative DTI, MRI results indicate that untreated deep tissue injuries are on the scale of multiple cm [2]. Thus, being able to detect lesions of at least 1 cm in diameter should prove to be adequate to both detect and monitor DTI. [c1]

In order to investigate the effect of lesion depth on the detection sensitivity, measured strain ratios for circular lesions with a diameter of 2.5 cm located at various depths were interrogated with a 4 MHz probing frequency, and strained by 5 %. The results of this investigation are seen in Fig. 3.9.

In Fig. 3.21, it can be seen there there was little interplay between detection sensitivity and measured strain ratios at the various depths examined for all but the case for very soft (mushy) lesions (with a stiffness ratio of 0.32). At such low stiffness ratios, the excessive tissue deformation interrupts the tissue strain estimation algorithm's ability to adequately track the induced displacements in the lesion.

[c1] *KH*: Included discussion about detection ability for small lesions

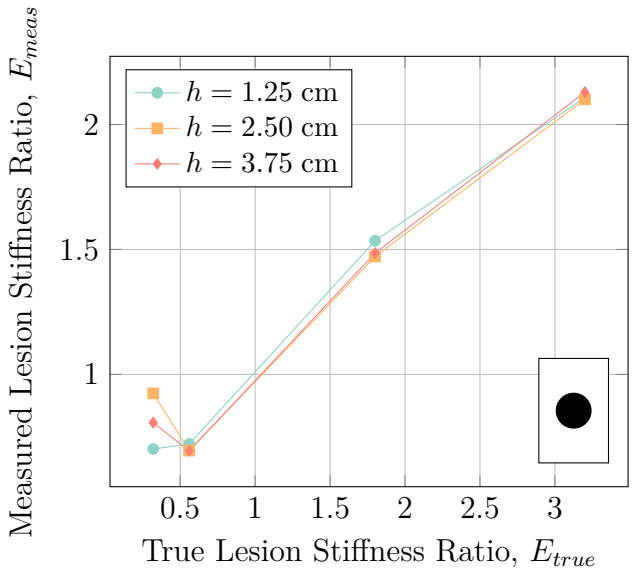

Figure 3.10: Effect of lesion altitude above the underlying bone. Aside from erroneous results at very low lesion stiffness ratios, the effect is negligible.

Since the strain field caused by compressive forces near an extremely rigid structure embedded within a relatively soft domain will be significantly heterogeneous, the effect of lesion altitude above the underlying stiff bone was examined with the hypothesis that if the lesion were too close to the hard bone, it would be masked by the strain field caused by the bone's existence. A 2.5 cm diameter lesion was interrogated with a 4 MHz probing frequency and 5 % applied strain. The results of this characterization are given in Fig. 3.10.

In Fig. 3.10, it can be seen that the lesion altitude above the underlying bone had very little effect on the detection sensitivity. Although larger strain fields may be generated near the bone, it is hypothesized that the larger fields also extend larger and so affect healthy tissue to more or less the same degree as the forming lesion.

In order to characterize the effect of using alternate ultrasound probing frequencies, simulations were carried out on lesions using probing frequencies of 2 MHz, 4 MHz, and 8 MHz. The simulated lesions had a diameter of 2.5 cm,

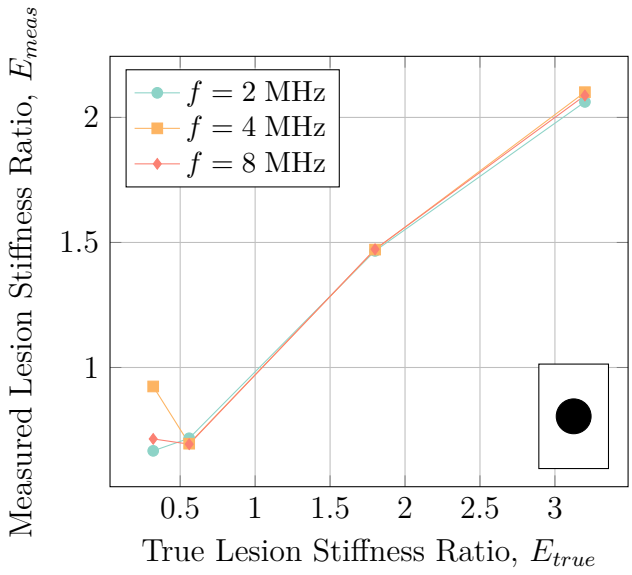

Figure 3.11: Characterization of ultrasonic probing frequency on detection sensitivity. Apart from the requirement of using an ultrasonic frequency low enough to interrogate the desired tissue, probing frequency has negligible effect on the detection sensitivity.

were located at a depth of 10 cm and we strain at 5 %. The results of this study are given in Fig. 3.11.

As can be seen from Fig. 3.11, there is very little effect on the detection sensitivity from the ultrasound probing frequency that was used, therefore an appropriate frequency should be chosen so as to reach the the full depth of the bone-muscle interface at suspected DTI locations [c1]while retaining the best image resolution.

As quasi-static ultrasound elastography is most likely to be performed via manual indentation where the exact magnitude of applied deformation is unknown, it is important to study the effect of applied strain magnitude on the detection sensitivity. Applied strains of 2.5 %, 5.0 %, and 10 % were investigated on a 2.5 cm diameter lesion at a depth of 10 cm using a probing frequency of 4 MHz; the results are given in Fig. 3.12.

[c1] *MFP: Text added.*

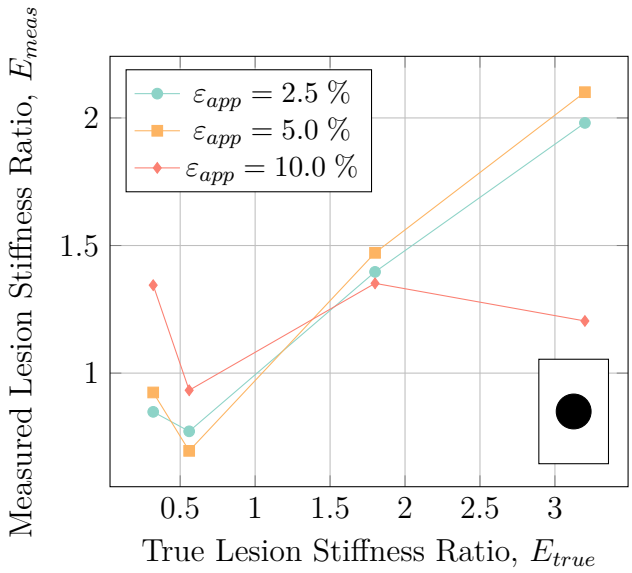

Figure 3.12: Applied strain characterization plot for lesions with a diamater of 2.5 cm located at a depth of 10 cm interrogated at 4 MHz. There is little difference between 2.5 % and 5.0 % applied strain, while large-magnitude strains of 10 % generate significant error for both very soft and very stiff lesions.

While Fig. 3.12 shows a relatively constant detection sensitivity for compressive strains of 2.5 % and 5 %, compressive strains of 10 % generate significant measurement error for both very soft and very stiff lesions. Under large compressive strains, the tissue (either in the lesion as in the soft lesion case, or the surrounding tissue as in the stiff lesion case) deforms considerably which again interferes with the algorithm's ability to properly track the displacement of tissue. It should also be noted that applying overly large strains to an already forming deep tissue injury may cause additional unwarranted damage. Thus it is imperative that applied surface indentation be kept to reasonable bounds ($2.5 - 5$ %, or $0.25 - 0.50$ cm in 10 cm deep domains), not only for safety of the tissue but also for clarity of the diagnostic test.

To study the effect that closely spaced lesions will have on the detection sensitivity as well as how discernible the lesions will be from each other, the separation distance between two 1.0 cm diameter co-located lesions at a depth

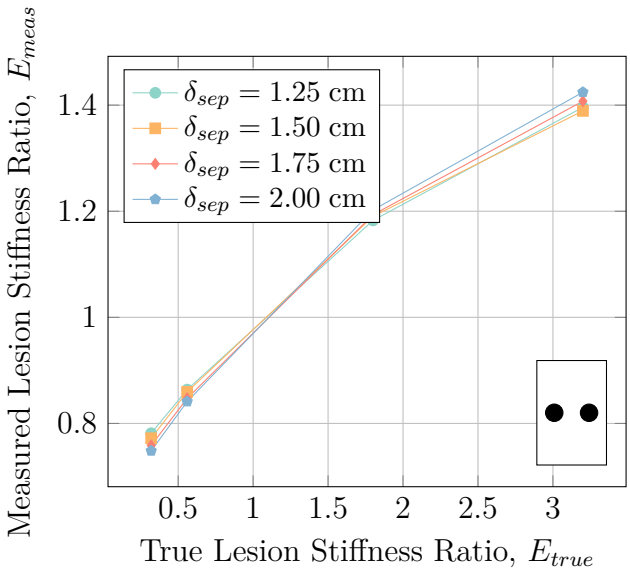

Figure 3.13: Effect of lesion separation distance on two 1.0 cm diameter lesions co-located at a depth of 10 cm interrogated with a 4 MHz probe with 5 % applied strain. There is no negligible difference between separation distances on the detection sensitivity.

of 10 cm was examined using a 4 MHz probing frequency with 5 % applied strain magnitude. The results of this study are shown in 3.13.

While Fig. 3.13 shows that the separation distance between co-located lesions causes a negligible effect on the detection sensitivity, Fig. 3.14 shows regions of decreased strain above and below the centreline of the lesions. While these regions had the same basal stiffness as the bulk tissue, the decreased strain pattern may obfuscate the true results by introducing "phantom lesions" which are not actually present but merely the result of the existing lesions.

While the simulations performed thus far assumed that lesions were perfect spheres with hard boundaries in order to isolate specific parameters of interest, this assumption may not always be accurate. Rather, due to the nature of injury formation, lesions may form gradual boundaries that "fade" from stiff or necrotic tissue to healthy tissue. To investigate the effect of this phenomenon on the detection sensitivity, lesions with "blurred boundaries" were investi-

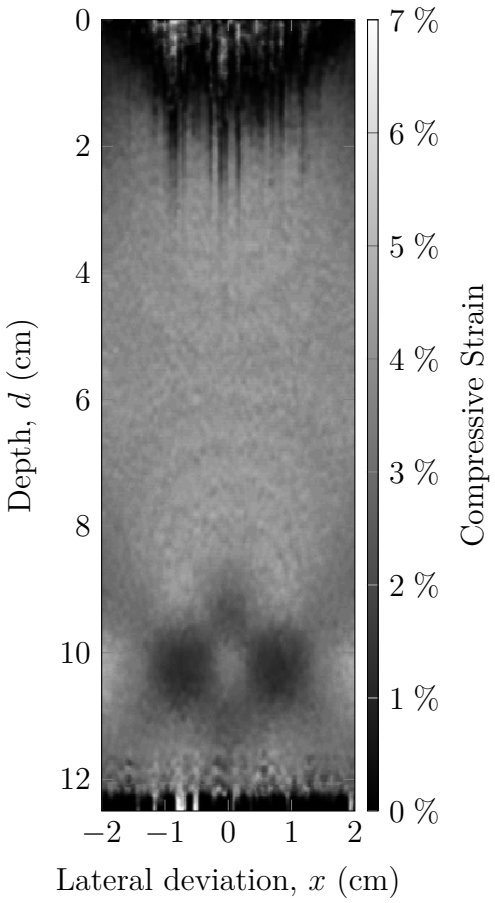

Figure 3.14: Elastogram for two co-located lesions of 1.0 cm diameter at a depth of 10 cm interrogated using a 4 MHz probing frequency with 5 % applied strain. A pattern of decreased strain is present above and below the centerline between the two lesions while the lesions themselves are not affected by each other.

gated. Hard spherical lesions were blurred by convolving the lesion domain with a disc blurring kernel of varying radius. The results for this investigation on lesions with a diameter of 2.5 cm, at a depth of 10 cm and interrogated with a 4 MHz probing frequency with 5 % applied strain are given in Fig. 3.15.

Fig. 3.15 shows that there is very little dependence on the lesion detection sensitivity for stiff lesions (lesions with a stiffness ratio ≥ 1.0). However, for soft lesions, the tissue strain estimation algorithm seems to over-estimate the stiffness of the lesions.

Similar to how lesions may have "blurred boundaries" rather that hard

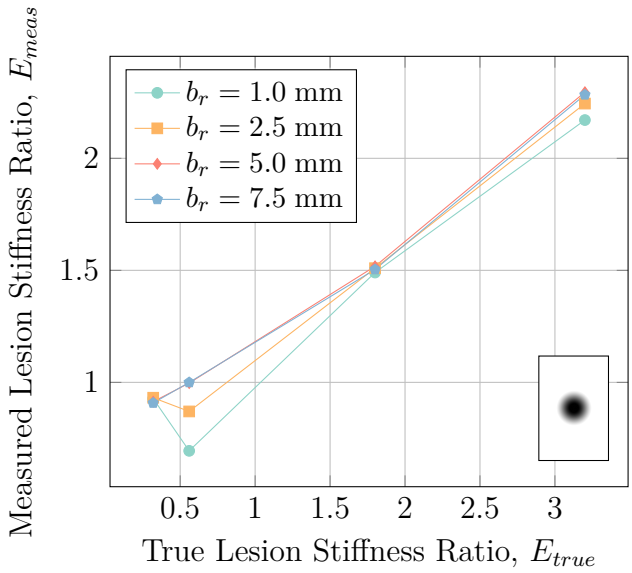

Figure 3.15: Characterization of the effect of lesion blur radius on lesion detection sensitivity for a 2.5 cm diameter lesion at a depth of 10 cm using a probing frequency of 4 MHz and applied strain of 5 %. While there is negligible effect of the blur radius on stiff lesions, the strain ratio for soft lesions is considerably over-estimated.

ones, so too may lesion composition not be homogeneous. In order to study the effect of heterogeneous regions of injured tissue, the detection sensitivity of a set of numerous small lesions located within close proximity to each other so as to form a large, heterogeneous area of diseased tissue was examined. Fig. 3.16 shows the results for this model for varying numbers of 2 mm diameter lesions in a 2.5 cm diameter circle located at a depth of 10 cm with a probing frequency of 4 MHz and 5 % applied strain. Fig. 3.18 further explores this model by investigating the case where there are 30 small lesions per square cm with individual lesions ranging in diameter from 0.5 mm to 1.5 mm.

The characterization plot in Fig. 3.16 for small lesion density is less linear than other characterization plots, with lesion density having a significant effect on the detection sensitivity. Specifically, for low lesion densities, the detection sensitivity is much lower than for high lesion densities. However, this observation is warranted after examination of the elastogram produced from these

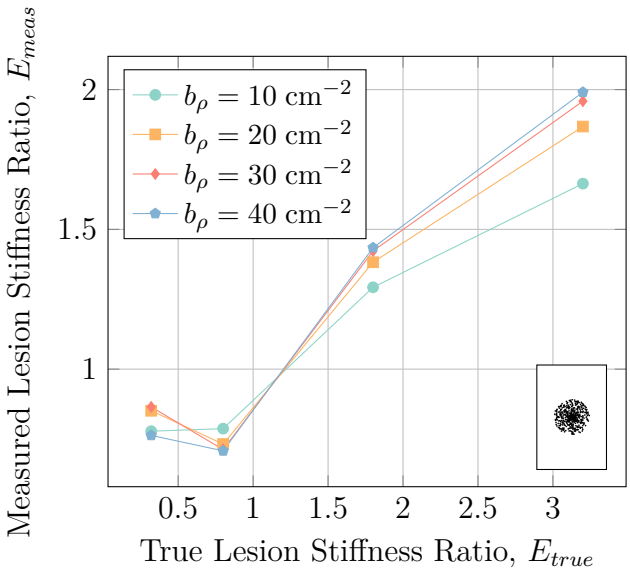

Figure 3.16: Characterization of lesion density for a group of numerous smaller 2 mm diameter lesions comprising a large area with a diameter of 2.5 cm at a depth of 10 cm interrogated with a 4 MHz probing frequency and 5 % applied strain. Detection sensitivity decreases with decreasing lesion density, as expected.

results, given in Fig. 3.17, which shows how the small lesions are not individually detected but rather the entire region is detected as one large lesion. Since the average stiffness ratio over this region is lesser than the stiffness ratio of individual lesions, it makes sense that the "measured" strain ratio will be less than expected.

Similar to the results shown in Fig. 3.16, changing the size of the individual small lesions does have an effect on the measured strain. In this case, when individual lesions are small, the total area occupied by lesions is lesser which results in a lesser average tissue stiffness over the grouped lesion region.

[c1]Note that although the elastography algorithm was able to detect the larger lesion-filled regions in these simulations, it was completely unable to discern the individual lesions comprising those regions. This is not surprising due to both the generated strain fields in the healthy tissue throughout the

[c1] *KH*: Included discussion about detection ability of localized lesion properties

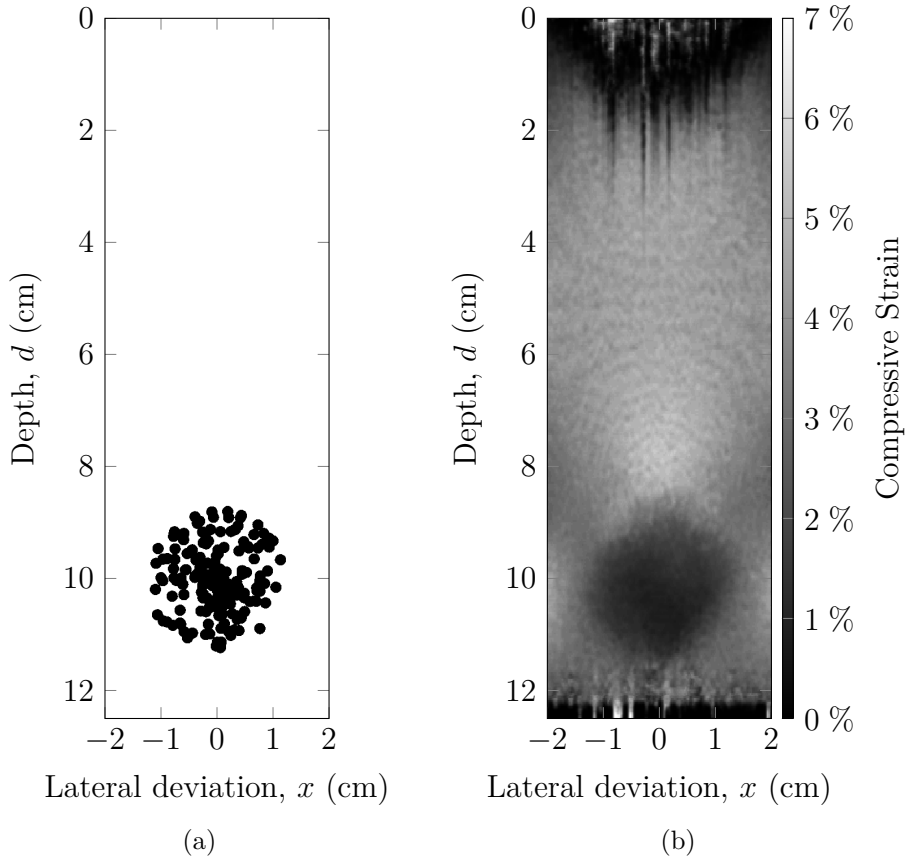

Figure 3.17: Stiffness map (a) and corresponding elastogram (b) for a group a small lesions with a density of 10 lesions per cm^2 grouped in a 2.5 cm diameter circle at a depth of 10 cm interrogated with a 4 MHz probing frequency and 5 % applied strain. In (a), white regions are regular tissue while black regions are the small lesions. In the elastogram, individual lesions do not stand out, rather the entire region of lesions appears as one large region of unhealthy tissue.

larger lesion area as well as the results presented in Fig. 3.8 showing poor detection sensitivity for lesions with diameters $\leq$ 1 cm while the individual lesions in this simulation had diameters of the scale of 0.5 mm – 1.5 mm.

Finally, in order to place these results within the context of a likely real scenario in humans, a more complicated model utilizing an MRI-acquired lesion and slides from the Visible Human Project [1] was developed. Specifically, lesion geometry was taken from a real deep tissue injury in a pig model imaged using T_2^*-weighted MRI. The human geometry was taken from a transverse

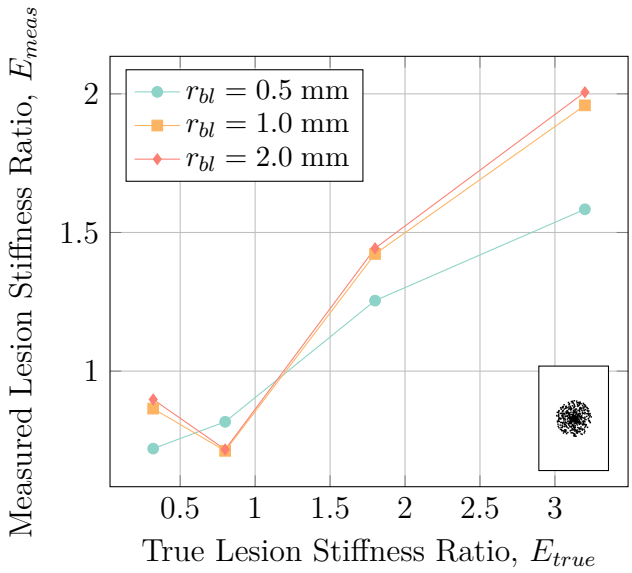

Figure 3.18: Characterization of lesion radius for a group of numerous smaller lesions with a density of 30 lesions per cm^2 comprising a large area with a diameter of 2.5 cm at a depth of 10 cm interrogated with a 4 MHz probing frequency and 5 % applied strain. Detection sensitivity decreases with decreasing individual lesion size, as expected.

plane slice aross the left ischial tuberosity such that the lesion was placed immediately superficial to the boney promience. For this model, the overall lesion width and lesion depth were examined with results shown in Figs. 3.19 and 3.21 respectively.

In Fig. 3.19, it is clear to see than small lesions (with a diameter ≤ 1.0 cm) are almost impossible to adequately detect (although larger lesions will be adequately detectable). It is hypothesized that this phenomenon is due to the excessive strain apparent above the boney prominence that is seen in the resultant elastogram given in Fig. 3.20 such that the lesion is "washed out" by the strain field developed by the relatively stiff bone nearby.

In Fig. 3.21, there is little to no dependence of the detection sensitivity on the lesion depth in the Visible Human-MRI model with all depth curves displaying the same profile. However, deeper lesions (lesions closer to the bony prominence) have stiffnesses that are over-estimated with respect to their

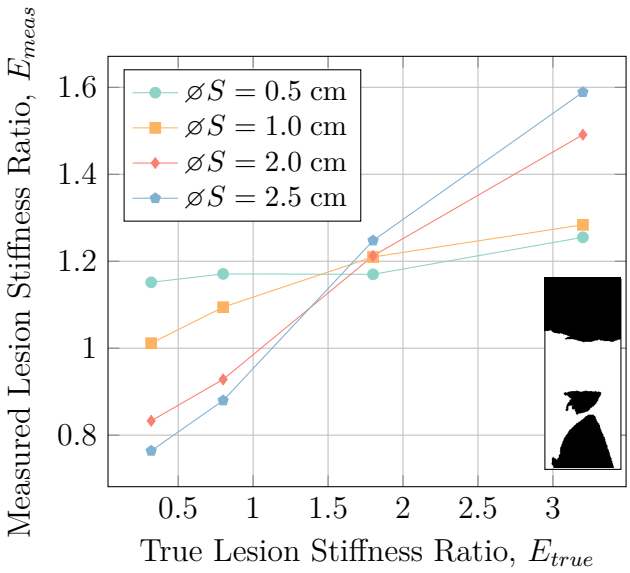

Figure 3.19: Characterization of lesion width in a Visible Human-MRI model for lesions at a depth of 7.25 cm interrogated with a 4 MHz probing frequency with 5 % applied strain. Small lesions (with a width $\leq$ 1.0 cm) are severely misrepresented and portray general over-estimation of lesion stiffness larger lesions.

superficial counterparts. This is hypothesized to be due to the increased strain field present in all of the soft tissue located immediately superior to the bony prominence, but should not pose a serious problem for imaging lesions of this nature.

3.3.4 Physical Phantom Validation

In order to ensure that the models presented here represented physical realities, a small subset of the cases studied were modelled in a physical phantom, specifically for three lesions with stiffness ratios of 0.56, 1.80, and 3.20 with a diameter of 2.0 cm and at a depth of 3.5 cm, interrogated at 8 MHz with approximately 5 % applied strain. The results of this study are summarized in Fig. 3.22.

As can be seen in Fig. 3.22, a relatively simple (although inexact) rela-

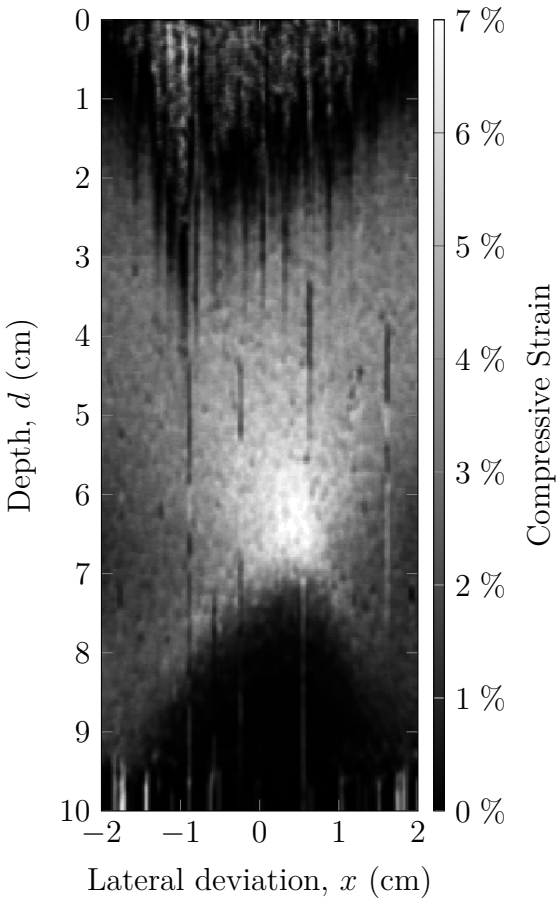

Figure 3.20: Elastogram for a 0.5 cm wide lesion embedded in the Visible Human-MRI model domain at a depth of 7.25 cm interrogated at 4 MHz with an applied strain of 2.5 %. The lesion is not visible and is the resultant elastogram.

tionship between simulated and experimental measured strain ratios exists. It must be noted that the finite-element simulations of b-mode image formation and tissue deformation presented here are idealizations of reality and idealization errors such as the ultrasound pulse profile and plane-strain assumption no doubt contributed to the difference seen in Fig. 3.22.

It must be noted that in order to acquire quasi-static elastography results in the physical phantom, the ultrasound transducer was required to be manually manipulated to cause indentation in the phantom, as the technique would most likely be performed in a clinical setting. This was found to be problematic as

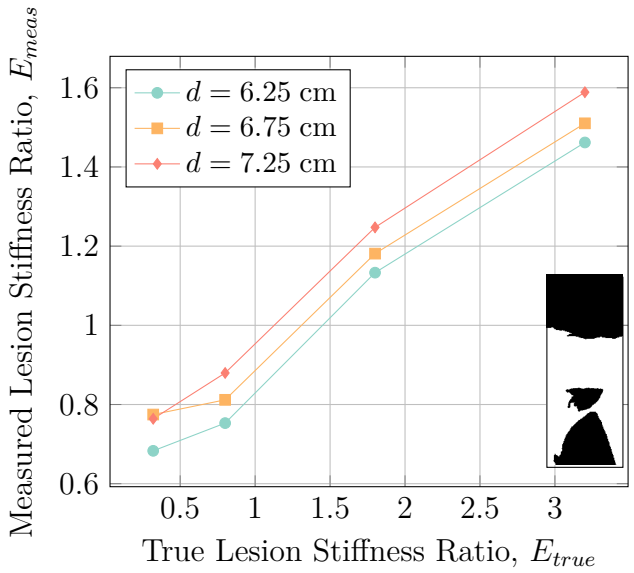

Figure 3.21: Characterization of lesion depth in a Visible Human-MRI model for lesions with a width of 2.5 cm interrogated with a 4 MHz probing frequency and 5 % applied strain. Deeper lesions (closer to the bony promience) are have slightly over-estimated lesion stiffness ratios as opposed to more superficial lesions while detection sensitivity is not affected by lesion depth.

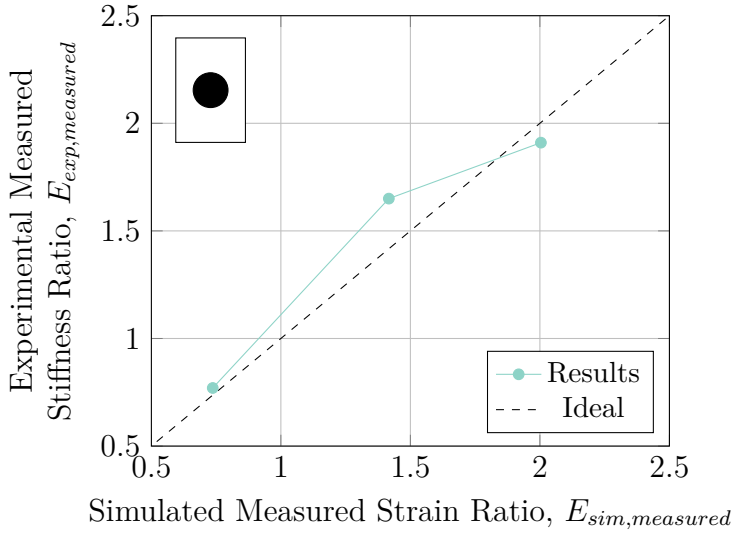

Figure 3.22: Relation between simulated measured strain ratios and experimental measured strain ratios for a lesion at a depth of 3.5 cm and diameter of 2.0 cm showing general agreement between simulated and experimental cases. Idealization errors are the most likely the cause of the differences seen between simulated and experimental cases.

the ultrasound transducer was difficult to maintain perfectly perpendicular and in-plane during the compression (largely due to the necessity of using coupling ultrasonic gel). This difficulty suggests that acoustic radiation force impulse (ARFI) elastography would be a more appropriate method to acquire DTI elastograms. ARFI elastography works on the same principles as quasi-static elastography with the exception that tissue deformation is caused by localized large-amplitude acoustic waves generated by the transducer such that human factors play a far less substantial role in image acquisition.

3.4 Conclusions

With this work, we presented a numerical characterization of the use of quasi-static ultrasound elastography for the early detection of deep tissue injuries (DTI). There is a real clinical need for an objective tool that is capable of detecting the formation and progression of DTI in human subjects as these wounds are generally not visible from the surface of the skin until they have broken through and already caused substantial damage.

[c1]Through our numerical characterization, quasi-static ultrasound elastography was found to be an effective tool for detecting and monitoring DTI in theoretical simulations. Overall, detection sensitivity was less than expected. Small lesions (with diameters ≤ 1.0 cm) were more difficult to [c2]differentiate due to the low lesion detection sensitivity. While lesion depth, altitude above the underlying bone, and probing frequency did not have significant effect on the lesion detection sensitivity, it was found that applying high levels of compressive strain (10 %) introduced severe error for both very soft and very stiff lesions, thus it is recommended that diagnosticians only apply moder-

[c1] *KH*: Updated conclusions to reflect new models and data
[c2] *MFP*: ~~detect~~

ate ($\leq$ 5 %) compressive strain when interrogating potential lesions. In the more complicated model of co-located lesions, while the separation distance between adjacent lesions did not affect the detection sensitivity, the placing of adjacent lesions generated "phantom" lesion regions with altered strain that may appear to be diseased tissue when they are in fact healthy. In a model lesion with gradual blurred boundaries, the effect of blur radius only affected the detection sensitivity and ability to [c3]differentiate soft lesions. Specifically, soft lesions with large blur radii became nearly impossible to [c4]differentiate. In the case of numerous clustered small lesions, both decreased lesion density and decreased individual lesion size caused a decrease in lesion detection sensitivity, likely due to the averaging effect of healthy tissue and diseased tissue in near proximity. Finally, in the Visible Human-MRI acquired lesion model, lesions with widths $\leq$ 1.0 cm are nearly impossible to [c5]differentiate as they are hidden by the strain field generated by the bony prominence. Lesion depth did not have an effect on the detection sensitivity, though deeper lesions (lesions which were closer to the bony prominence) had overestimated stiffnesses with respect to their more superficial counterparts.

A subset of the results found through simulation were compared with similar experiments done using a tissue mimicking phantom model. The experimental results using the phantom model generally agreed with those found from simulation cases. It was also noted that the manual skin indentation technique involved with quasi-static ultrasound elastography proved to be difficult to produce reliable images. This difficulty suggests that an alternate method of performing ultrasound elastography may be preferable to quasi-static ultrasound elastography with manual indentation. Acoustic radiation force im-

[c3] *MFP*: ~~detect~~
[c4] *MFP*: ~~detect~~
[c5] *MFP*: ~~detect~~

pulse (ARFI) elastography may be a more appropriate method to acquire DTI elastograms as although ARFI elastography works on the same principles as quasi-static elastography, the difference lays in the fact that tissue deformation is caused by localized large-amplitude acoustic waves generated by the transducer. This means that human factors play a far less substantial role in image acquisition and would likely improve repeatability and inter-operator reliability. Nevertheless, the work done here to characterize the use of quasi-static ultrasound elastography is an important step along the path of generating a useful clinical tool for detecting formative and monitoring progressive deep tissue injuries.

References

[1] T. U. S. National Library of Medicine, *Visible human project*, 1994.

[2] L. R. Solis, E. Twist, P. Seres, R. B. Thompson, and V. K. Mushahwar, "Prevention of deep tissue injury through muscle contractions induced by intermittent electrical stimulation after spinal cord injury in pigs.," *Journal of applied physiology (Bethesda, Md. : 1985)*, vol. 114, no. 2, pp. 286–296, Jan. 15, 2013, ISSN: 1522-1601. DOI: 10.1152/japplphysiol.00257.2012. [Online]. Available: http://dx.doi.org/10.1152/japplphysiol.00257.2012.

[3] J. C. Bamber and R. J. Dickinson, "Ultrasonic b-scanning: a computer simulation.," *Physics in medicine and biology*, vol. 25, no. 3, pp. 463–479, May 1980, ISSN: 0031-9155. [Online]. Available: http://view.ncbi.nlm.nih.gov/pubmed/7403261.

[4] T. A. Krouskop, T. M. Wheeler, F. Kallel, B. S. Garra, and T. Hall, "Elastic moduli of breast and prostate tissues under compression," *Ultrasonic Imaging*, vol. 20, no. 4, pp. 260–274, Oct. 1, 1998, ISSN: 1096-0910. DOI: 10.1177/016173469802000403. [Online]. Available: http://dx.doi.org/10.1177/016173469802000403.

[5] A. P. Choi and Y. P. Zheng, "Estimation of young's modulus and poisson's ratio of soft tissue from indentation using two different-sized indentors: finite element analysis of the finite deformation effect.," *Medical & biological engineering & computing*, vol. 43, no. 2, pp. 258–264, Mar. 2005, ISSN: 0140-0118. [Online]. Available: http://view.ncbi.nlm.nih.gov/pubmed/15865137.

[6] A. D. Martin, M. Z. Daniel, D. T. Drinkwater, and J. P. Clarys, "Adipose tissue density, estimated adipose lipid fraction and whole body adiposity

in male cadavers.," *International journal of obesity and related metabolic disorders : journal of the International Association for the Study of Obesity*, vol. 18, no. 2, pp. 79–83, Feb. 1994, ISSN: 0307-0565. [Online]. Available: http://view.ncbi.nlm.nih.gov/pubmed/8148928.

[7] E. Brusseau, J. Kybic, J.-F. F. Deprez, and O. Basset, "2-D locally regularized tissue strain estimation from radio-frequency ultrasound images: theoretical developments and results on experimental data.," *IEEE transactions on medical imaging*, vol. 27, no. 2, pp. 145–160, Feb. 2008, ISSN: 0278-0062. DOI: 10.1109/tmi.2007.897408. [Online]. Available: http://dx.doi.org/10.1109/tmi.2007.897408.

Chapter 4

Numerical Characterization of Acoustic Radiation Force Impulse Imaging

4.1 Introduction

Lorem ipsum dolor sit amet, consectetuer adipiscing elit. Ut purus elit, vestibulum ut, placerat ac, adipiscing vitae, felis. Curabitur dictum gravida mauris. Nam arcu libero, nonummy eget, consectetuer id, vulputate a, magna. Donec vehicula augue eu neque. Pellentesque habitant morbi tristique senectus et netus et malesuada fames ac turpis egestas. Mauris ut leo. Cras viverra metus rhoncus sem. Nulla et lectus vestibulum urna fringilla ultrices. Phasellus eu tellus sit amet tortor gravida placerat. Integer sapien est, iaculis in, pretium quis, viverra ac, nunc. Praesent eget sem vel leo ultrices bibendum. Aenean faucibus. Morbi dolor nulla, malesuada eu, pulvinar at, mollis ac, nulla. Curabitur auctor semper nulla. Donec varius orci eget risus. Duis nibh mi, congue eu, accumsan eleifend, sagittis quis, diam. Duis eget orci sit amet orci

dignissim rutrum.

4.2 Methods

Lorem ipsum dolor sit amet, consectetuer adipiscing elit. Ut purus elit, vestibulum ut, placerat ac, adipiscing vitae, felis. Curabitur dictum gravida mauris. Nam arcu libero, nonummy eget, consectetuer id, vulputate a, magna. Donec vehicula augue eu neque. Pellentesque habitant morbi tristique senectus et netus et malesuada fames ac turpis egestas. Mauris ut leo. Cras viverra metus rhoncus sem. Nulla et lectus vestibulum urna fringilla ultrices. Phasellus eu tellus sit amet tortor gravida placerat. Integer sapien est, iaculis in, pretium quis, viverra ac, nunc. Praesent eget sem vel leo ultrices bibendum. Aenean faucibus. Morbi dolor nulla, malesuada eu, pulvinar at, mollis ac, nulla. Curabitur auctor semper nulla. Donec varius orci eget risus. Duis nibh mi, congue eu, accumsan eleifend, sagittis quis, diam. Duis eget orci sit amet orci dignissim rutrum.

4.2.1 Numerical Model

Lorem ipsum dolor sit amet, consectetuer adipiscing elit. Ut purus elit, vestibulum ut, placerat ac, adipiscing vitae, felis. Curabitur dictum gravida mauris. Nam arcu libero, nonummy eget, consectetuer id, vulputate a, magna. Donec vehicula augue eu neque. Pellentesque habitant morbi tristique senectus et netus et malesuada fames ac turpis egestas. Mauris ut leo. Cras viverra metus rhoncus sem. Nulla et lectus vestibulum urna fringilla ultrices. Phasellus eu tellus sit amet tortor gravida placerat. Integer sapien est, iaculis in, pretium quis, viverra ac, nunc. Praesent eget sem vel leo ultrices bibendum. Aenean faucibus. Morbi dolor nulla, malesuada eu, pulvinar at, mollis ac, nulla.

Curabitur auctor semper nulla. Donec varius orci eget risus. Duis nibh mi, congue eu, accumsan eleifend, sagittis quis, diam. Duis eget orci sit amet orci dignissim rutrum.

Governing Equations

The governing equations use for this model were the set of coupled first-order partial differential equations 4.1. These equations are the first-order equivalents of 4.2 taking into account acoustic absorption, tissue heterogeneities, and acoustic wave non-linearities **treeby12**

$$\nabla^2 p - \frac{1}{c_0^2} \frac{\partial^2 p}{\partial t^2} = 0 \tag{4.2}$$

Boundary and Initial Conditions

Lorem ipsum dolor sit amet, consectetuer adipiscing elit. Ut purus elit, vestibulum ut, placerat ac, adipiscing vitae, felis. Curabitur dictum gravida mauris. Nam arcu libero, nonummy eget, consectetuer id, vulputate a, magna. Donec vehicula augue eu neque. Pellentesque habitant morbi tristique senectus et netus et malesuada fames ac turpis egestas. Mauris ut leo. Cras viverra metus rhoncus sem. Nulla et lectus vestibulum urna fringilla ultrices. Phasellus eu tellus sit amet tortor gravida placerat. Integer sapien est, iaculis in, pretium quis, viverra ac, nunc. Praesent eget sem vel leo ultrices bibendum. Aenean faucibus. Morbi dolor nulla, malesuada eu, pulvinar at, mollis ac, nulla. Curabitur auctor semper nulla. Donec varius orci eget risus. Duis nibh mi, congue eu, accumsan eleifend, sagittis quis, diam. Duis eget orci sit amet orci dignissim rutrum.

4.3 Results

Lorem ipsum dolor sit amet, consectetuer adipiscing elit. Ut purus elit, vestibulum ut, placerat ac, adipiscing vitae, felis. Curabitur dictum gravida mauris. Nam arcu libero, nonummy eget, consectetuer id, vulputate a, magna. Donec vehicula augue eu neque. Pellentesque habitant morbi tristique senectus et netus et malesuada fames ac turpis egestas. Mauris ut leo. Cras viverra metus rhoncus sem. Nulla et lectus vestibulum urna fringilla ultrices. Phasellus eu tellus sit amet tortor gravida placerat. Integer sapien est, iaculis in, pretium quis, viverra ac, nunc. Praesent eget sem vel leo ultrices bibendum. Aenean faucibus. Morbi dolor nulla, malesuada eu, pulvinar at, mollis ac, nulla. Curabitur auctor semper nulla. Donec varius orci eget risus. Duis nibh mi, congue eu, accumsan eleifend, sagittis quis, diam. Duis eget orci sit amet orci dignissim rutrum.

Chapter 5

Numerical Characterization of Shear Wave Speed Quantification

Lorem ipsum dolor sit amet, consectetuer adipiscing elit. Ut purus elit, vestibulum ut, placerat ac, adipiscing vitae, felis. Curabitur dictum gravida mauris. Nam arcu libero, nonummy eget, consectetuer id, vulputate a, magna. Donec vehicula augue eu neque. Pellentesque habitant morbi tristique senectus et netus et malesuada fames ac turpis egestas. Mauris ut leo. Cras viverra metus rhoncus sem. Nulla et lectus vestibulum urna fringilla ultrices. Phasellus eu tellus sit amet tortor gravida placerat. Integer sapien est, iaculis in, pretium quis, viverra ac, nunc. Praesent eget sem vel leo ultrices bibendum. Aenean faucibus. Morbi dolor nulla, malesuada eu, pulvinar at, mollis ac, nulla. Curabitur auctor semper nulla. Donec varius orci eget risus. Duis nibh mi, congue eu, accumsan eleifend, sagittis quis, diam. Duis eget orci sit amet orci dignissim rutrum.

Chapter 6

Conclusion

Lorem ipsum dolor sit amet, consectetuer adipiscing elit. Ut purus elit, vestibulum ut, placerat ac, adipiscing vitae, felis. Curabitur dictum gravida mauris. Nam arcu libero, nonummy eget, consectetuer id, vulputate a, magna. Donec vehicula augue eu neque. Pellentesque habitant morbi tristique senectus et netus et malesuada fames ac turpis egestas. Mauris ut leo. Cras viverra metus rhoncus sem. Nulla et lectus vestibulum urna fringilla ultrices. Phasellus eu tellus sit amet tortor gravida placerat. Integer sapien est, iaculis in, pretium quis, viverra ac, nunc. Praesent eget sem vel leo ultrices bibendum. Aenean faucibus. Morbi dolor nulla, malesuada eu, pulvinar at, mollis ac, nulla. Curabitur auctor semper nulla. Donec varius orci eget risus. Duis nibh mi, congue eu, accumsan eleifend, sagittis quis, diam. Duis eget orci sit amet orci dignissim rutrum.

6.1 Clinical Need for DTI Detection

Lorem ipsum dolor sit amet, consectetuer adipiscing elit. Ut purus elit, vestibulum ut, placerat ac, adipiscing vitae, felis. Curabitur dictum gravida mauris. Nam arcu libero, nonummy eget, consectetuer id, vulputate a, magna. Donec

vehicula augue eu neque. Pellentesque habitant morbi tristique senectus et netus et malesuada fames ac turpis egestas. Mauris ut leo. Cras viverra metus rhoncus sem. Nulla et lectus vestibulum urna fringilla ultrices. Phasellus eu tellus sit amet tortor gravida placerat. Integer sapien est, iaculis in, pretium quis, viverra ac, nunc. Praesent eget sem vel leo ultrices bibendum. Aenean faucibus. Morbi dolor nulla, malesuada eu, pulvinar at, mollis ac, nulla. Curabitur auctor semper nulla. Donec varius orci eget risus. Duis nibh mi, congue eu, accumsan eleifend, sagittis quis, diam. Duis eget orci sit amet orci dignissim rutrum.

6.2 USE Provides Potential Diagnosis Capability

Lorem ipsum dolor sit amet, consectetuer adipiscing elit. Ut purus elit, vestibulum ut, placerat ac, adipiscing vitae, felis. Curabitur dictum gravida mauris. Nam arcu libero, nonummy eget, consectetuer id, vulputate a, magna. Donec vehicula augue eu neque. Pellentesque habitant morbi tristique senectus et netus et malesuada fames ac turpis egestas. Mauris ut leo. Cras viverra metus rhoncus sem. Nulla et lectus vestibulum urna fringilla ultrices. Phasellus eu tellus sit amet tortor gravida placerat. Integer sapien est, iaculis in, pretium quis, viverra ac, nunc. Praesent eget sem vel leo ultrices bibendum. Aenean faucibus. Morbi dolor nulla, malesuada eu, pulvinar at, mollis ac, nulla. Curabitur auctor semper nulla. Donec varius orci eget risus. Duis nibh mi, congue eu, accumsan eleifend, sagittis quis, diam. Duis eget orci sit amet orci dignissim rutrum.

6.3 Future Work

Lorem ipsum dolor sit amet, consectetuer adipiscing elit. Ut purus elit, vestibulum ut, placerat ac, adipiscing vitae, felis. Curabitur dictum gravida mauris. Nam arcu libero, nonummy eget, consectetuer id, vulputate a, magna. Donec vehicula augue eu neque. Pellentesque habitant morbi tristique senectus et netus et malesuada fames ac turpis egestas. Mauris ut leo. Cras viverra metus rhoncus sem. Nulla et lectus vestibulum urna fringilla ultrices. Phasellus eu tellus sit amet tortor gravida placerat. Integer sapien est, iaculis in, pretium quis, viverra ac, nunc. Praesent eget sem vel leo ultrices bibendum. Aenean faucibus. Morbi dolor nulla, malesuada eu, pulvinar at, mollis ac, nulla. Curabitur auctor semper nulla. Donec varius orci eget risus. Duis nibh mi, congue eu, accumsan eleifend, sagittis quis, diam. Duis eget orci sit amet orci dignissim rutrum.

6.3.1 Animal Studies?

Lorem ipsum dolor sit amet, consectetuer adipiscing elit. Ut purus elit, vestibulum ut, placerat ac, adipiscing vitae, felis. Curabitur dictum gravida mauris. Nam arcu libero, nonummy eget, consectetuer id, vulputate a, magna. Donec vehicula augue eu neque. Pellentesque habitant morbi tristique senectus et netus et malesuada fames ac turpis egestas. Mauris ut leo. Cras viverra metus rhoncus sem. Nulla et lectus vestibulum urna fringilla ultrices. Phasellus eu tellus sit amet tortor gravida placerat. Integer sapien est, iaculis in, pretium quis, viverra ac, nunc. Praesent eget sem vel leo ultrices bibendum. Aenean faucibus. Morbi dolor nulla, malesuada eu, pulvinar at, mollis ac, nulla. Curabitur auctor semper nulla. Donec varius orci eget risus. Duis nibh mi, congue eu, accumsan eleifend, sagittis quis, diam. Duis eget orci sit amet orci

dignissim rutrum.

6.3.2 Human Studies?

Lorem ipsum dolor sit amet, consectetuer adipiscing elit. Ut purus elit, vestibulum ut, placerat ac, adipiscing vitae, felis. Curabitur dictum gravida mauris. Nam arcu libero, nonummy eget, consectetuer id, vulputate a, magna. Donec vehicula augue eu neque. Pellentesque habitant morbi tristique senectus et netus et malesuada fames ac turpis egestas. Mauris ut leo. Cras viverra metus rhoncus sem. Nulla et lectus vestibulum urna fringilla ultrices. Phasellus eu tellus sit amet tortor gravida placerat. Integer sapien est, iaculis in, pretium quis, viverra ac, nunc. Praesent eget sem vel leo ultrices bibendum. Aenean faucibus. Morbi dolor nulla, malesuada eu, pulvinar at, mollis ac, nulla. Curabitur auctor semper nulla. Donec varius orci eget risus. Duis nibh mi, congue eu, accumsan eleifend, sagittis quis, diam. Duis eget orci sit amet orci dignissim rutrum.

Appendix A

Data Tables

Lorem ipsum dolor sit amet, consectetuer adipiscing elit. Ut purus elit, vestibulum ut, placerat ac, adipiscing vitae, felis. Curabitur dictum gravida mauris. Nam arcu libero, nonummy eget, consectetuer id, vulputate a, magna. Donec vehicula augue eu neque. Pellentesque habitant morbi tristique senectus et netus et malesuada fames ac turpis egestas. Mauris ut leo. Cras viverra metus rhoncus sem. Nulla et lectus vestibulum urna fringilla ultrices. Phasellus eu tellus sit amet tortor gravida placerat. Integer sapien est, iaculis in, pretium quis, viverra ac, nunc. Praesent eget sem vel leo ultrices bibendum. Aenean faucibus. Morbi dolor nulla, malesuada eu, pulvinar at, mollis ac, nulla. Curabitur auctor semper nulla. Donec varius orci eget risus. Duis nibh mi, congue eu, accumsan eleifend, sagittis quis, diam. Duis eget orci sit amet orci dignissim rutrum.

A.1 Quasi-Static Ultrasound Elastography

Lorem ipsum dolor sit amet, consectetuer adipiscing elit. Ut purus elit, vestibulum ut, placerat ac, adipiscing vitae, felis. Curabitur dictum gravida mauris. Nam arcu libero, nonummy eget, consectetuer id, vulputate a, magna. Donec

vehicula augue eu neque. Pellentesque habitant morbi tristique senectus et netus et malesuada fames ac turpis egestas. Mauris ut leo. Cras viverra metus rhoncus sem. Nulla et lectus vestibulum urna fringilla ultrices. Phasellus eu tellus sit amet tortor gravida placerat. Integer sapien est, iaculis in, pretium quis, viverra ac, nunc. Praesent eget sem vel leo ultrices bibendum. Aenean faucibus. Morbi dolor nulla, malesuada eu, pulvinar at, mollis ac, nulla. Curabitur auctor semper nulla. Donec varius orci eget risus. Duis nibh mi, congue eu, accumsan eleifend, sagittis quis, diam. Duis eget orci sit amet orci dignissim rutrum.

A.2 Acoustic Radiation Force Impulse Imaging

Lorem ipsum dolor sit amet, consectetuer adipiscing elit. Ut purus elit, vestibulum ut, placerat ac, adipiscing vitae, felis. Curabitur dictum gravida mauris. Nam arcu libero, nonummy eget, consectetuer id, vulputate a, magna. Donec vehicula augue eu neque. Pellentesque habitant morbi tristique senectus et netus et malesuada fames ac turpis egestas. Mauris ut leo. Cras viverra metus rhoncus sem. Nulla et lectus vestibulum urna fringilla ultrices. Phasellus eu tellus sit amet tortor gravida placerat. Integer sapien est, iaculis in, pretium quis, viverra ac, nunc. Praesent eget sem vel leo ultrices bibendum. Aenean faucibus. Morbi dolor nulla, malesuada eu, pulvinar at, mollis ac, nulla. Curabitur auctor semper nulla. Donec varius orci eget risus. Duis nibh mi, congue eu, accumsan eleifend, sagittis quis, diam. Duis eget orci sit amet orci dignissim rutrum.

A.3 Shear Wave Speed Quantification

Lorem ipsum dolor sit amet, consectetuer adipiscing elit. Ut purus elit, vestibulum ut, placerat ac, adipiscing vitae, felis. Curabitur dictum gravida mauris. Nam arcu libero, nonummy eget, consectetuer id, vulputate a, magna. Donec vehicula augue eu neque. Pellentesque habitant morbi tristique senectus et netus et malesuada fames ac turpis egestas. Mauris ut leo. Cras viverra metus rhoncus sem. Nulla et lectus vestibulum urna fringilla ultrices. Phasellus eu tellus sit amet tortor gravida placerat. Integer sapien est, iaculis in, pretium quis, viverra ac, nunc. Praesent eget sem vel leo ultrices bibendum. Aenean faucibus. Morbi dolor nulla, malesuada eu, pulvinar at, mollis ac, nulla. Curabitur auctor semper nulla. Donec varius orci eget risus. Duis nibh mi, congue eu, accumsan eleifend, sagittis quis, diam. Duis eget orci sit amet orci dignissim rutrum.

Appendix B

Source Code

Lorem ipsum dolor sit amet, consectetuer adipiscing elit. Ut purus elit, vestibulum ut, placerat ac, adipiscing vitae, felis. Curabitur dictum gravida mauris. Nam arcu libero, nonummy eget, consectetuer id, vulputate a, magna. Donec vehicula augue eu neque. Pellentesque habitant morbi tristique senectus et netus et malesuada fames ac turpis egestas. Mauris ut leo. Cras viverra metus rhoncus sem. Nulla et lectus vestibulum urna fringilla ultrices. Phasellus eu tellus sit amet tortor gravida placerat. Integer sapien est, iaculis in, pretium quis, viverra ac, nunc. Praesent eget sem vel leo ultrices bibendum. Aenean faucibus. Morbi dolor nulla, malesuada eu, pulvinar at, mollis ac, nulla. Curabitur auctor semper nulla. Donec varius orci eget risus. Duis nibh mi, congue eu, accumsan eleifend, sagittis quis, diam. Duis eget orci sit amet orci dignissim rutrum.

B.1 Quasi2DUltrasound

Lorem ipsum dolor sit amet, consectetuer adipiscing elit. Ut purus elit, vestibulum ut, placerat ac, adipiscing vitae, felis. Curabitur dictum gravida mauris. Nam arcu libero, nonummy eget, consectetuer id, vulputate a, magna. Donec

vehicula augue eu neque. Pellentesque habitant morbi tristique senectus et netus et malesuada fames ac turpis egestas. Mauris ut leo. Cras viverra metus rhoncus sem. Nulla et lectus vestibulum urna fringilla ultrices. Phasellus eu tellus sit amet tortor gravida placerat. Integer sapien est, iaculis in, pretium quis, viverra ac, nunc. Praesent eget sem vel leo ultrices bibendum. Aenean faucibus. Morbi dolor nulla, malesuada eu, pulvinar at, mollis ac, nulla. Curabitur auctor semper nulla. Donec varius orci eget risus. Duis nibh mi, congue eu, accumsan eleifend, sagittis quis, diam. Duis eget orci sit amet orci dignissim rutrum.